Supplementary Information (SI) for Green Chemistry.
This journal is © The Royal Society of Chemistry 2026

Supporting Information (SI)

Fe(II)-Organic Frameworks as Heterogeneous Catalysts for Achieving Diverse CO_2 Conversions

Tian-Cai Yue, Xin-Fang Wang, Jian-Bo Huang, Lu-Lu Wang and Duo-Zhi Wang*

General Method

All solvents and chemicals were directly used without further purification. Powder X-ray diffraction (PXRD) spectra were performed by Bruker D8 diffractometer. Flourier transform infrared spectroscopy (FT-IR) was measured on a Bruker Equinox 55 using the KBr pellet in the range of 4000-400 cm^{-1}. Thermogravimetric analyses (TGA) were carried out on a Hitachi STA200 simultaneous thermal analyzer at a heating rate of 10 ^{o}C/min from room temperature to 800 ^{o}C in N_2 atmosphere. BET surface area has been recorded using nitrogen sorption data at 77 K with a volumetric adsorption setup (Micromeritics ASAP 2460 instruments). CO_2 adsorption-desorption isotherm measurements on a Quantachrome Autosorb-iQ at 273 K and 298 K. ^{1}H NMR spectra were recorded on Bruker AVANCE III HD 600 spectrometer (Bruker BioSpin, Rheinstetten, Germany). Inductively coupled plasma−optical emission spectroscopy (ICP−OES) analysis was measured by PerkinElmer Optima 8000. Single-crystal XRD data of crystal was measured on a Bruker APEX II CCD diffractometer with graphite-monochromated Mo Kα radiation (λ = 0.71073 Å) at 296 K. The MOFs structure is solved directly by structural solvers Olex2 [1] and SIR2004 [2] and refined with the ShelXL [3] refinement package using Least Squares minimization. The detailed crystallographic information of the crystal was listed in Table S1. The selected bond distances and bond angles were listed in Table S2. The CCDC number of MOFs **1** and **2** are 2470183 and 2470184, respectively. These data can be obtained from the CCDC via www.ccdc.cam.ac.uk/data_request/cif. The ligand H_2**L^1** (5-(1*H*-1,2,4-triazol-1-yl)isophthalic acid) and H_2**L^2** (5-(1*H*-imidazol-1-yl)isophthalic acid) were synthesized according to the reported procedure and the ligands structure are shown in **Scheme S1**.[4]

Synthesis of MOF 1 ($\{[Fe_2L^1_2(H_2O)_4]\cdot H_2O\}_n$ (1))

$FeSO_4\cdot 7H_2O$ (0.0278 g, 0.1 mmol) and H_2**L^1** (0.02332 g, 0.1 mmol) mixed solvents V_{H2O}: $V_{CH3CH2OH}$: V_{DMA} = 5:3:2) were added to a 20 mL Teflon-lined stainless-steel autoclave, heated at 160 °C for 12 h, then cooled to room temperature. The yellow massive crystals were collected by filtration and washed with methanol (calcd 41% yield based on ligand H_2**L^1**). IR (KBr, cm^{-1}): 3145(w), 1625(s, COO^-), 1582(s, Ph C=C), 1545(m, triazole C=N), 1485(m), 1434(s), 1378(s), 1352(w, COO^-), 1294(w), 1214(m), 1145(m), 1076(m), 984(m), 900(m), 771(m), 750(m), 721(m), 668(m), 526(w)(Fe-N/Fe-O) (Fig. S2a).

Synthesis of MOF 2 ($[FeL^2(H_2O)_2]_n$ (2))

$FeSO_4 \cdot 7H_2O$ (0.0278 g, 0.1 mmol) and $H_2\mathbf{L^2}$ (0.02322 g, 0.1 mmol) mixed solvents V_{H2O}: $V_{CH3CH2OH}$: V_{DMA} = 7:4:5) were added to a 20 mL Teflon-lined stainless-steel autoclave, heated at 160 °C for 12 h, then cooled to room temperature. The gellow massive crystals were collected by filtration and washed with methanol (calcd 31% yield based on ligand $H_2\mathbf{L^2}$). IR (KBr, cm^{-1}): 3140(w), 1633(s, COO^-), 1582(s, imidazole C=N), 1535(w, Ph C=C), 1471(w), 1430(m), 1381(s, COO^-), 1313(w), 1265(m), 1173(w), 1072(s), 945(m), 898(w), 775(s), 744(s), 717(s), 650(w), 523(w)(Fe-N/Fe-O) (Fig. S2a).

Table S1. Crystallographic data and structure refinement details for MOFs **1** and **2**.

Data.	MOF **1**	MOF **2**
Formula	$C_{20}H_{20}Fe_2N_6O_{13}$	$C_{11}H_{12}FeN_2O_6$
Mr	664.12	324.06
crystal system	Monoclinic	Monoclinic
space group	*C*2/*c*	$P2_1/c$
a (Å)	19.612(16)	10.758(2)
b (Å)	10.811(7)	16.767(4)
c (Å)	13.532(11)	7.3771(17)
α (°)	90	90
β (°)	123.86(3)	95.384(14)
γ (°)	90	90
V($Å^3$)	2383(3)	1324.8(5)
Z	4	4
ρ_{calc} (mg/m^3)	1.851	1.615
μ (mm^{-1})	1.303	9.410
F(000)	1352	656.0
θ range(°)	2.261-25.078	8.256-133.714
Reflns collected	19749	2327
GOF on F^2	1.227	0.954
R^a/wR^b	0.0387/0.1284	0.1218/0.2793

Table S2. Selected bond distances (Å) and angles (°) for MOFs **1** and **2**.

MOF **1**			
Fe(1)-O(3)	2.019(3)	Fe(1)-O(1)#2	2.229(3)
Fe(1)-N(3)#1	2.161(3)	N(3)-Fe(1)#3	2.161(3)
Fe(1)-O(5)	2.181(3)	O(1)-Fe(1)#4	2.229(3)
Fe(1)-O(6)	2.181(3)	O(2)-Fe(1)#4	2.206(3)
Fe(1)-O(2)#2	2.206(3)	N(3)#1-Fe(1)-O(2)#2	146.48(11)
O(3)-Fe(1)-N(3)#1	94.69(13)	O(5)-Fe(1)-O(2)#2	88.30(12)
O(3)-Fe(1)-O(5)	87.90(12)	O(6)-Fe(1)-O(2)#2	88.29(12)
N(3)#1-Fe(1)-O(5)	95.82(12)	O(3)-Fe(1)-O(1)#2	175.62(11)
O(3)-Fe(1)-O(6)	92.95(12)	N(3)#1-Fe(1)-O(1)#2	87.82(12)
N(3)#1-Fe(1)-O(6)	87.52(13)	O(5)-Fe(1)-O(1)#2	88.28(11)
O(5)-Fe(1)-O(6)	176.48(10)	O(6)-Fe(1)-O(1)#2	90.73(12)
O(3)-Fe(1)-O(2)#2	118.73(11)	O(2)#2-Fe(1)-O(1)#2	58.99(10)
MOF **2**			
Fe(1)-(N2)#1	2.101(8)	Fe(1)-(O6)	2.067(7)
Fe(1)-(O2)	2.067(7)	N(2)-Fe(1)#3	2.101(8)
Fe(1)-(O3)#2	2.357(7)	O(3)-Fe(1)#4	2.357(7)
Fe(1)-(O4)#2	2.182(7)	O(4)-Fe(1)#4	2.182(7)
Fe(1)-(O5)	2.071(7)	(O4)#2-Fe(1)-(O3)#2	57.7(2)
(N2)#1- Fe(1)-(O3)#2	151.7(3)	(O5)-Fe(1) (N2)#1	95.6(3)
(N2)#1-Fe(1)-(O4)#2	94.1(3)	(O5)-Fe(1)-(O3)#2	86.1(3)
(O2)-Fe(1)-(N2)#1	95.4(3)	(O5)-Fe(1)-(O4)#2	89.4(3)
(O2)-Fe(1)-(O3)#2	112.9(3)	(O6)-Fe(1)-(N2)#1	95.9(3)
(O2)-Fe(1)-(O4)#2	170.5(3)	(O6)-Fe(1)-(O3)#2	85.1(3)
(O2)-Fe(1)-(O5)	88.3(3)	(O6)-Fe(1)-(O4)#2	92.5(3)
(O2)-Fe(1)-(O5)	87.9(3)	(O6)-Fe(1)-(O5)	168.2(3)

Symmetry codes: For **MOF 1**：#1 x,y+1,z #2 x+1/2,-y+3/2,z+1/2, #3 x,y-1,z, #4 x-1/2,-y+3/2,z-1/2.

For **MOF 2**：#1 -1+X, +Y, +Z #2 -X, 1/2+Y, 1/2-Z, #3 1+X, +Y, +Z, #4 -X, -1/2+Y, 1/2-Z.

Table S3. Crystallographic data and structure refinement details for MOF **1**@1a, MOF **1**@3a and MOF **1**@5a.

Data.	MOF **1**@1a	MOF **1**@3a	MOF **1**@5a
Formula	$C_{10}H_9FeN_3O_6$	$C_{10}H_9FeN_3O_6$	$C_{10}H_9FeN_3O_6$
Mr	323.05	323.05	323.05
crystal system	Monoclinic	Monoclinic	Monoclinic
space group	*C*2/*c*	*C*2/*c*	*C*2/*c*
a (Å)	19.5951(6)	19.5983(14)	19.576(12)
b (Å)	10.8299(3)	10.8261(7)	10.830(3)
c (Å)	13.5113(8)	13.5151(10)	13.515(15)
α (°)	90	90	90
β (°)	123.9650(10)	124.045(3)	123.96(2)
γ (°)	90	90	90
V(Å^3)	2378.05(17)	2376.0(3)	2377(3)
Z	8	8	8
ρ_{calc} (mg/m^3)	1.805	1.806	1.806
μ (mm^{-1})	10.512	10.521	10.519
F(000)	1312.0	1312.0	1312.0
θ range(°)	9.814-133.002	9.818-133.638	9.816-133.238
Reflns collected	7360	8459	6757
GOF on F^2	1.051	1.060	1.063
R^a/wR^b	0.0815/0.2130	0.0679/0.1753	0.0482/0.1330

Table S4. Selected bond distances (Å) and angles (°) for MOF **1**@1a, MOF **1**@3a, and MOF **1**@5a.

MOF **1**@1a			
Fe1-N3#1	2.158(4)	Fe1-O6	2.181(4)
Fe1-O1#2	2.227(3)	N3-Fe1#3	2.159(4)
Fe1-O2#2	2.207(3)	O1-Fe1#4	2.227(3)
Fe1-O4	2.023(3)	O2-Fe1#4	2.207(3)
Fe1-O5	2.180(3)	N3#1-Fe1-O1#2	87.41(14)
N3#1-Fe1-O2#2	146.36(14)	N3#1-Fe1-O5	95.74(14)

N3#1-Fe1-O6	88.50(15)	O2#2-Fe1-O1#2	59.23(12)
O4-Fe1-N3#1	95.50(15)	O4-Fe1-O1#2	175.51(13)
O4-Fe1-O2#2	118.07(14)	O4-Fe1-O5	87.84(13)
O4-Fe1-O6	92.74(15)	O5-Fe1-O1#2	88.47(13)
O5-Fe1-O2#2	88.11(13)	O5-Fe1-O6	175.64(12)
O6-Fe1O-1#2	90.75(13)	O6-Fe1-O2#2	87.81(14)
		MOF **1**@3a	
Fe1-N3#1	2.156(3)	Fe1-O1#2	2.202(3)
Fe1-O2#2	2.225(3)	Fe1-O4	2.012(3)
Fe1-O5	2.191(4)	Fe1-O6	2.185(3)
N3-Fe1#3	2.156(3)	O1-Fe1#4	2.202(3)
O2-Fe1#4	2.225(3)	N3#1-Fe1-O12	146.31(12)
N3#1-Fe1-O2#2	87.51(12)	N31-Fe1-O5	87.81(13)
N31-Fe1-O6	95.98(13)	O1#2-Fe1-O2#2	59.12(10)
O4-Fe1-N3#1	95.22(13)	O4-Fe1-O1#2	118.38(12)
O4-Fe1-O2#2	175.73(12)	O4-Fe1-O5	92.76(13)
O4-Fe1-O6	87.90(13)	O5-Fe1-O1#2	88.07(12)
O5-Fe1-O2#2	90.62(12)	O6-Fe1-O1#2	88.22(11)
O6-Fe1-O2#2	88.55(11)	O6-Fe1-O5	176.08(10)
		MOF **1**@5a	
Fe1-N3#1	2.159(3)	Fe1-O2	87.46(12)
Fe1-O3#2	2.203(3)	Fe1-O4#2	2.227(2)
Fe1-O5	2.179(3)	Fe1-O6	2.178(3)
N3-Fe1#3	2.159(3)	O3-Fe1#4	2.203(3)
O4-Fe1#4	2.227(2)	N3#1-Fe1-O3#2	146.54(9)
N3#1-Fe1-O4#2	87.51(10)	N3#1-Fe1-O5	95.94(11)
N3#1-Fe1-O6	88.20(11)	O2-Fe1-N3#1	95.05(11)
O2-Fe1-O3#2	118.33(9)	O2-Fe1-O4#2	175.67(9)
O2-Fe1-O5	87.87(10)	O2-Fe1-O6	92.86(11)
O32-Fe1-O4#2	59.32(8)	O5-Fe1-O3#2	87.94(11)
O5-Fe1-O4#2	88.39(10)	O6-Fe1-O3#2	87.99(11)
O6-Fe1-O4#2	90.71(10)	O6-Fe1-O5	175.71(8)

Symmetry codes: For MOF **1**@1a: #1 +X,-1+Y, +Z, #2 1/2+X,1/2-Y,1/2+Z, #3 +X,1+Y,+Z, #4 -1/2+X,1/2-Y,-1/2+Z. For MOF **1**@3a: #1 +X,1+Y,+Z, #2 -1/2+X,3/2-Y,-1/2+Z, #3+X,-1+Y,+Z, #4 1/2+X,3/2-Y,1/2+Z. For MOF **1**@5a: #1 +X,1+Y,+Z, #2 -1/2+X,3/2-Y,-1/2+Z, #3 +X,-1+Y,+Z, #4

1/2+X,3/2-Y,1/2+Z.

Scheme S1. Structure of the ligands used in this work.

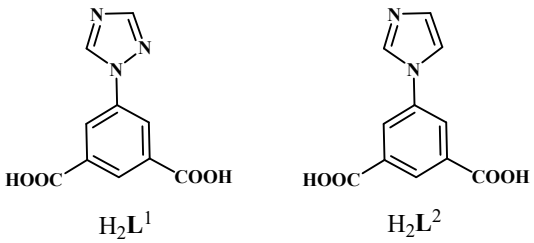

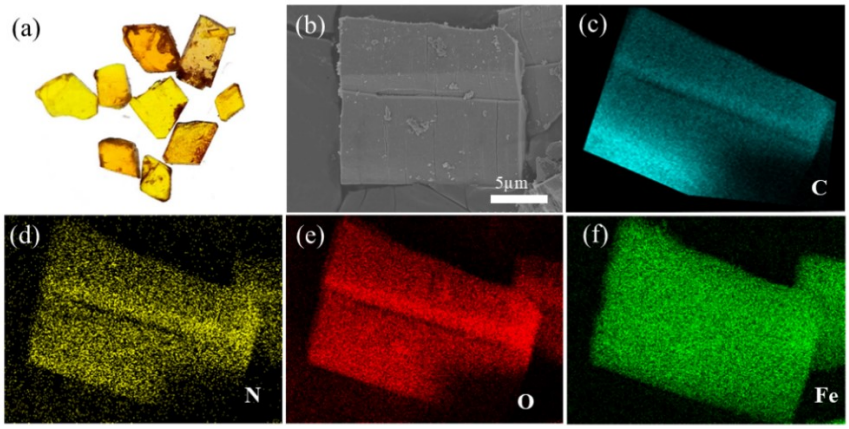

Fig. S1. (a) optical micrograph of MOF **2**. (b-f) SEM image and EDS elemental mapping of MOF **2**.

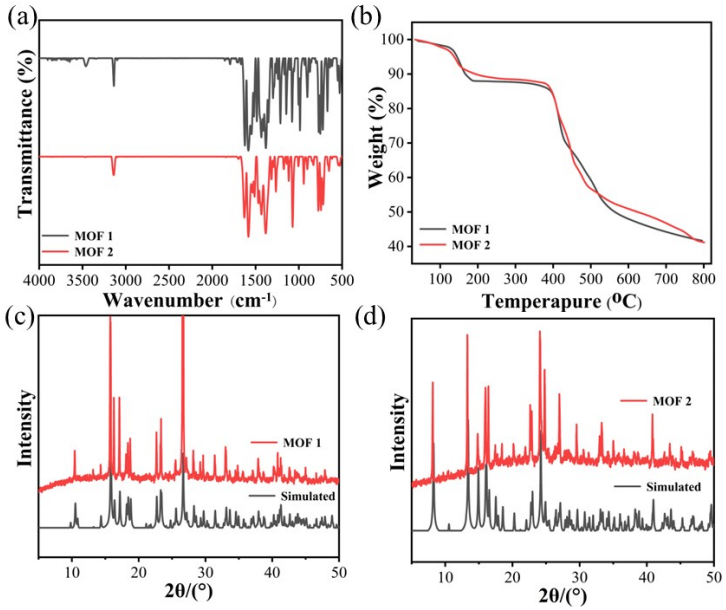

Fig. S2. (a) The FT-IR spectra. (b) TGA. (c-d) PXRD patterns of MOFs **1** and **2**.

Fig. S3. XPS spectra of MOFs **1** and **2**. (a) survey. (b) C 1s. (c) N 1s. (d) O 1s. (e) Fe 2p.

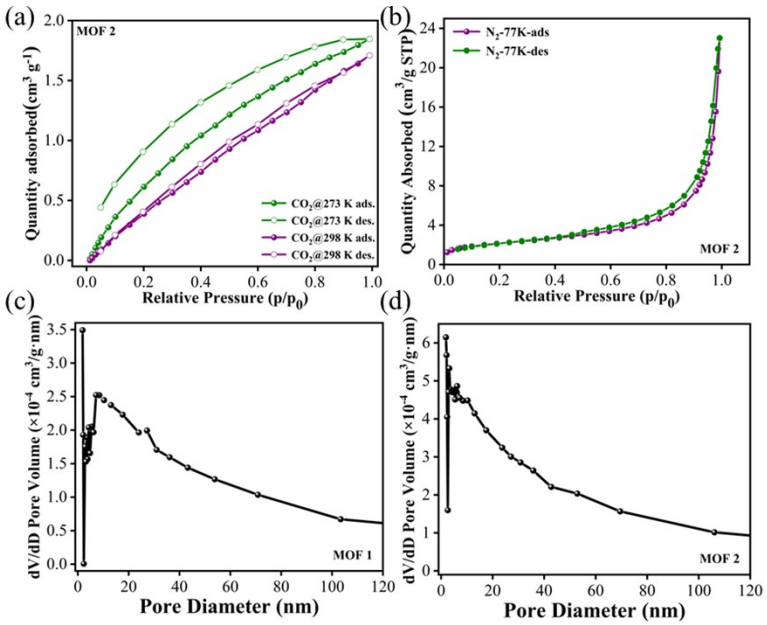

Fig. S4. (a-b) CO_2 and N_2 adsorption-desorption isotherm of MOF **2**. (c-d) The pore size distribution of MOFs **1** and **2**.

Procedure for catalytic carboxylation of terminal alkynes with CO_2.

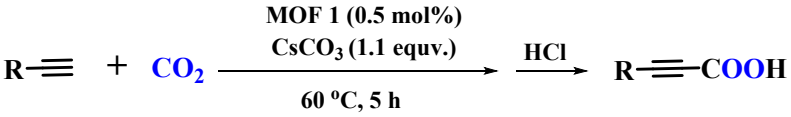

Scheme S2. General procedure for catalytic carboxylation of terminal alkynes with CO_2.

General procedure for catalytic carboxylation reactions of terminal alkynes by MOF 1: Typically, 0.5 mmol% MOF **1** and DMSO (1 mL) were carried out in a 10 mL Schlenk tube, then Cs_2CO_3 (1.1 equiv) and terminal alkyne (0.2 mmol) were added, and the reactor was flushed with CO_2 three times. Then, CO_2 was introduced and heated at 60 °C for 5 h. After reaction, 10 mL of H_2O was added, the catalyst was separated and the mixture was extracted with ethyl acetate (3×10 mL) to remove the organic phase. The H_2O phase was acidified with 1M HCl to pH = 1 and then extracted with ethyl acetate (3×40 mL). The organic phase was washed with saturated NaCl solution and dried over anhydrous $MgSO_4$. The product was further purified by column chromatography on silica gel (petroleum ether/ethyl acetate = 1:5 as an eluent) to afford pure product.

The cyclization reaction of epoxides with CO_2.

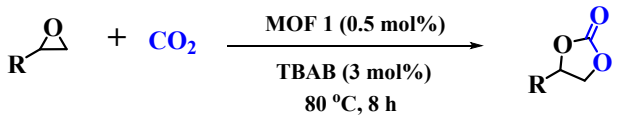

Scheme S3. General procedure for cyclization reaction of epoxides with CO_2.

General procedures for cyclization reaction of epoxides with CO_2 by MOF 1: Added 10 mmol

epoxides compound, 0.5 mmol% MOF **1** and 3 mmol% TBAB into the Schlenk bottle. The air in the Schlenk bottle was removed and 1 atm CO_2 was introduced into the Schlenk bottle, the reaction mixture was stirred at 80 ℃ for 8 h.

The cyclization reaction of propargylic amines with CO_2.

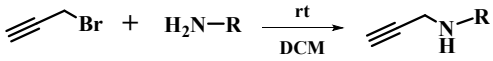

Scheme S4. General procedure for the synthesis of terminal propargylic amine (5a-5x).

General procedures for the synthesis of terminal propargylic amine: Propargylic bromide (5 mmol) was slowly added into amine (25 mmol) in dichloromethane (15 mL) over 30 minutes and the mixture was stirred overnight at room temperature. Then the mixture was extracted with dichloromethane and washed with saturated aqueous $NaHCO_3$ (3×20 mL) and the organic phases was collected and dried over anhydrous $MgSO_4$. The mixture was concentrated and purified by column chromatography on silica gel (petroleum ether/ethyl acetate = 9:1 as eluent) to afford the corresponding product as pale-yellow liquid.

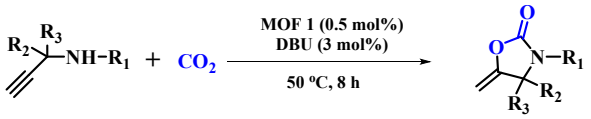

Scheme S5. General procedure for cyclization reaction of propargylic amine with CO_2.

General procedure for the carboxylative cyclization of propargylic amine with CO_2 catalyzed by MOF 1: In a typical experiment, the 0.5 mmol% MOF **1** and 1 mL CH_3CN were added into 10 mL Schlenk tube equipped with a magnetic stir bar, then propargylic amine (72.6 mg, 0.5 mmol), 1,8-diazabicyclo-[5.4.0]-undec-7-ene (DBU, 3 mol%) were added. Then 0.1 MPa of CO_2 was introduced and was stirred at 50 °C for 8 h. After reaction, the catalyst was separated and the mixture was extracted with ethyl acetate (3×20 mL) to collect the organic phase, washed with saturated NaCl solution and dried over anhydrous $MgSO_4$. The product was further purified by column chromatography on silica gel (petroleum ether/ethyl acetate = 10:1 as an eluent) to afford pure product.

Procedure for the recyclable experiment: In the recycling experiments, MOF **1** was separated by filtration, washed with methanol five times and then dried in a vacuum oven at 50 °C for 12 h for the next cycle test.

Kinetic investigation of CO_2 conversion: The impact of various factors on the conversion rates of

1a, 3a and 5a were experimentally proved through the investigate of reaction kinetics. In addition, the temperature-dependence of the reaction were explored to determine the reaction's activation energy. The kinetic equation was obtained based on the literature reports,[12] and it can be expressed as:

$$\ln(1\text{-}x) = -k_{obs}t + C \quad (1)$$

$$\ln K_{obs} = -E_a/RT + A \quad (2)$$

where k_{obs} is the rate constant, t is the reaction time (h), x is the 1a, 3a and 5a conversion (%), T is the temperature (K), A is the pre-exponential factor (s^{-1}), and E_a is the activation energy ($J \cdot mol^{-1}$).

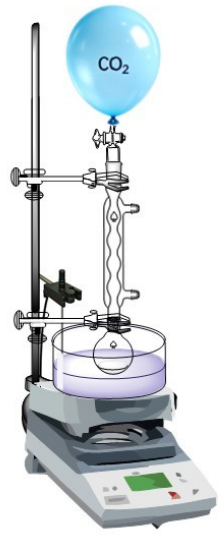

Fig. S5 Diagram of the reaction device.

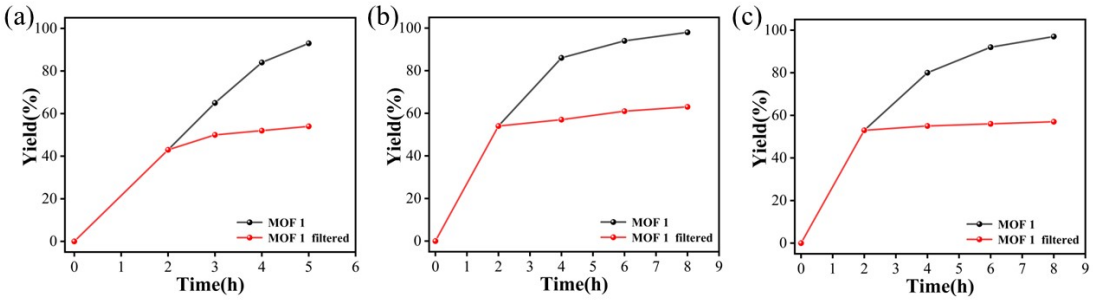

Fig. S6. (a-c) Evidence of heterogeneous nature of MOF **1** in the three CO_2 catalytic reaction: (a) carboxylation reaction of terminal alkynes with CO_2. (b) cycloaddition reaction of epoxides with CO_2. (c) carboxylative cyclization of propargylic amines with CO_2.

Fig. S7. First-order kinetic plots ln(1-x) versus time at different temperatures (a, d, g) MOF **1**. (b, e, h) MOF **2**. (c, f, j) fitted curves of ln*K*obs versus 1/T for carboxylation reaction of terminal alkynes with CO_2. cycloaddition reaction of epoxides with CO_2 and carboxylative cyclization of propargylic amines with CO_2, respectively.

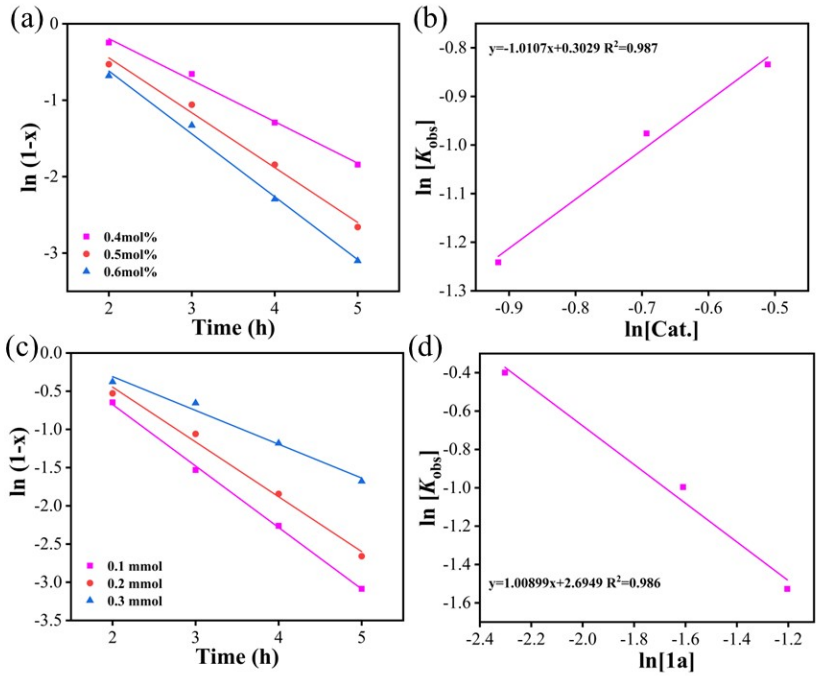

Fig. S8. First-order kinetics (ln(1-x) versus time) for (a) different catalyst dosage. (c) different amounts of substrates. (b, d) curve fitting of ln*K*obs against the ln[Cat.] and ln[1a] of carboxylation reaction of terminal alkynes with CO_2.

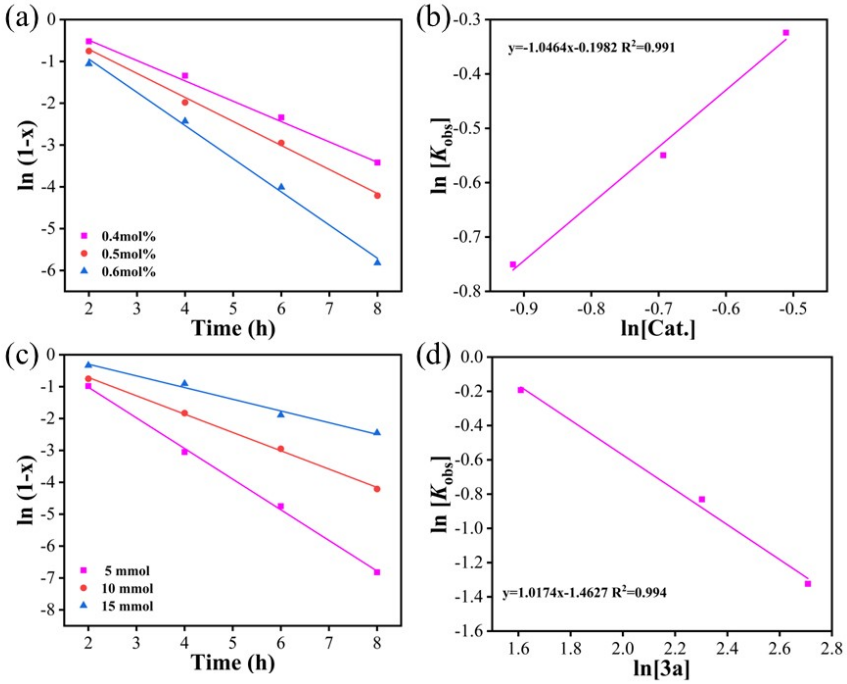

Fig. S9. First-order kinetics (ln(1-x) versus time) for (a) different catalyst dosage. (c) different amounts of substrates. (b, d) curve fitting of ln*K*obs against the ln[Cat.]and ln[3a] of cycloaddition reaction of epoxides with CO_2.

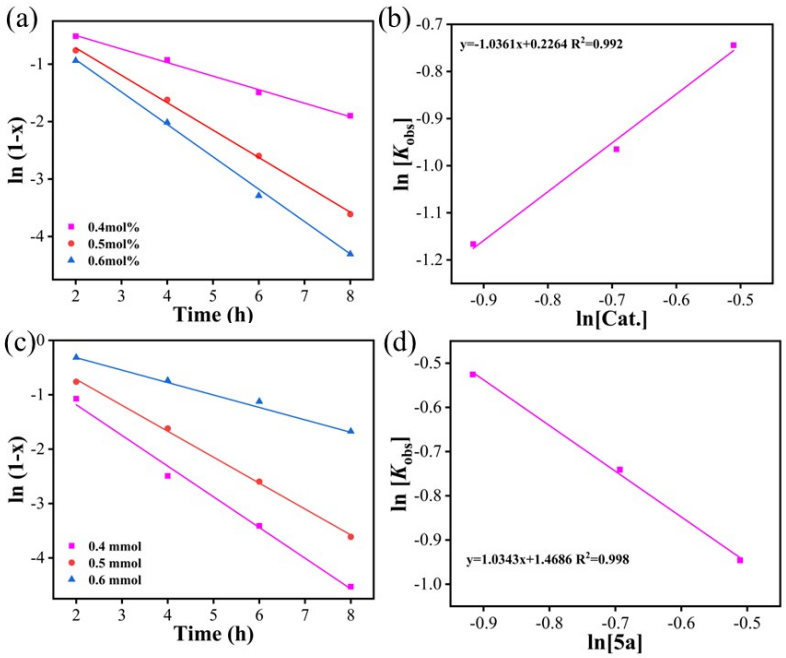

Fig. S10. First-order kinetics (ln(1-x) versus time) for (a) different catalyst dosage. (c) different amounts of substrates. (b, d) curve fitting of ln*K*obs against the ln[Cat.]and ln[5a] of carboxylative cyclization of propargylic amines with CO_2.

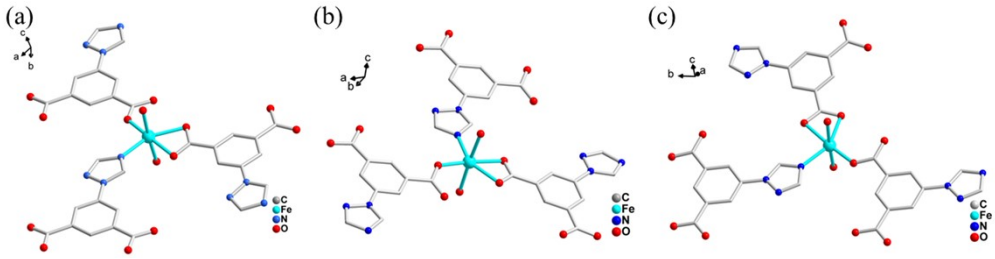

Fig. S11. (a-c) coordination environment of the Fe(II) ion of MOF **1@1a**, MOF **1@3a** and MOF **1@5a**.

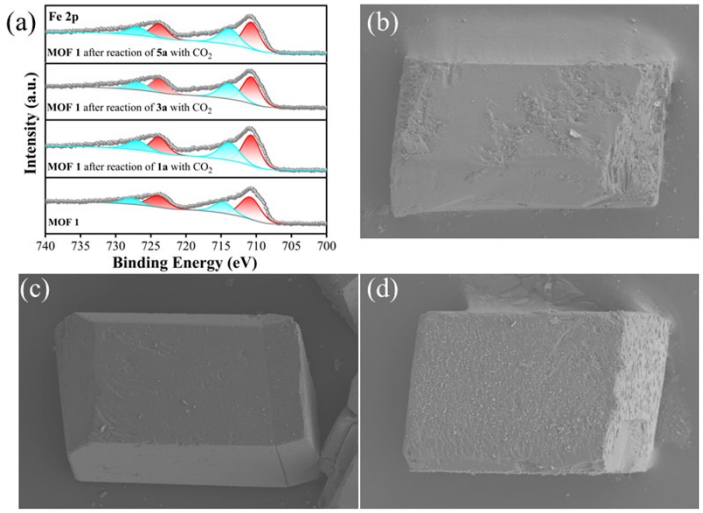

Fig. S12. Fe 2p and SEM images of MOF **1** after ten cycles in the three CO_2 catalytic reaction: (a) Fe 2p. (b) carboxylation reaction of terminal alkynes with CO_2. (c) cycloaddition reaction of

epoxides with CO_2. (d) carboxylative cyclization of propargylic amines with CO_2.

Table S5. Carboxylation reaction yields at different temperatures using MOFs **1** and **2** as catalysts.

Temperature (°C)	Yield (%)	
	MOF **1**	MOF **2**
50	82	64
60	93	80
70	95	89
80	97	94

Reaction conditions: substrate (0.2 mmol), 5 h, 0.1 MPa of CO_2.

Table S6. Cycloaddition reaction yields at different temperatures using MOFs **1** and **2** as catalysts.

Temperature (°C)	Yield (%)	
	MOF **1**	MOF **2**
60	89	56
70	95	76
80	98	89
90	99	96

Reaction conditions: substrate (10 mmol), 8 h, 0.1 MPa of CO_2.

Table S7. Carboxylative cyclization yields at different temperatures using MOFs **1** and **2** as catalysts.

Temperature (°C)	Yield (%)	
	MOF **1**	MOF **2**
40	93	71
50	97	84
60	98	93
70	99	97

Reaction conditions: substrate (0.5 mmol), 8 h, 0.1 MPa of CO_2.

Table S8. Carboxylation reaction yields of 1a with different catalyst dosages using MOF **1** as catalyst.

Catalyst dosage	Yield (%)

0.4 mol%	84
0.5 mol%	93
0.6 mol%	96

Reaction conditions: substrate (0.2 mmol), 60 °C, 5 h, 0.1 MPa of CO_2.

Table S9. Carboxylation reaction yields at different 1a dosages using MOF **1** as catalyst.

1a dosages	Yield (%)
0.1 mmol	95
0.2 mmol	93
0.3 mmol	81

Reaction conditions: 0.5 mol% Cat., 60 °C, 5 h, 0.1 MPa of CO_2.

Table S10. Cycloaddition reaction yields of 3a with different catalyst dosages using MOF **1** as catalyst.

Catalyst dosage	Yield (%)
0.4 mol%	94
0.5 mol%	98
0.6 mol%	99

Reaction conditions: substrate (10 mmol), 80 °C, 8 h, 0.1 MPa of CO_2.

Table S11. Cycloaddition reaction yields at different 3a dosages using MOF **1** as catalyst.

3a dosages	Yield (%)
5 mmol	99
10 mmol	98
15 mmol	88

Reaction conditions: 0.5 mol% Cat., 80 °C, 8 h, 0.1 MPa of CO_2.

Table S12. Carboxylative cyclization yields of 5a with different catalyst dosages using MOF **1** as catalyst.

Catalyst dosage	Yield (%)
0.4 mol%	85
0.5 mol%	97
0.6 mol%	99

Reaction conditions: substrate (0.5 mmol), 50 °C, 8 h, 0.1 MPa of CO_2.

Table S13. Carboxylative cyclization yields at different 5a dosages using MOF **1** as catalyst.

5a dosages	Yield (%)
0.4 mmol	99
0.5 mmol	97
0.6 mmol	82

Reaction conditions: 0.5 mol% Cat., 50 °C, 8 h, 0.1 MPa of CO_2.

Table S14. The performance comparison of carboxylation reaction of terminal alkynes with CO_2.

Materials	**Temp (°C)**	**Time (h)**	**Yield (%)**	**Ref.**
AgNPs/Co-MOF	80	14	98	5
Ag@Pybpy-COF	50	12	98	6
Cu(IN)-MOF	80	4	80	7
JNM-Au-1	50	2	90	8
Cu_2TCPP(M)	25	10	99	9
Ag/MIL-100(Fe)	50	12	92	10
Ag@MIL-100(Fe)	50	15	94.6	11
MOF **1**	50	5	93	This work

Table S15. The performance comparison of cycloaddition reaction of epoxides with CO_2.

Materials	**Temp (°C)**	**Time (h)**	**Yield (%)**	**Ref.**
Zn@PD-iCOF	100	12	99	12
MOCs	80	12	97	13
SiO_2@MOF	80	24	71	14
JLU-MOF200	60	6	58	15
Co-Py-COF	80	18	94	16
LCU-606	60	10	99	17
LTG-FeZr	120	8	90	18
MOF-919-Cu-Fe	25	24	99	19
$FeCo_2$-MOF	80	8	99	20

$Fe^{III}_4(Fe(CN)_6)_3$	100	3	99	21
MOF **1**	80	8	98	This work

Table S16. The performance comparison of carboxylative cyclization of propargylic amines with CO_2.

Materials	Temp (°C)	Time (h)	Yield (%)	Ref.
MOF (**1**)	50	12	99	22
Co-MOF	50	8	98	23
$[Zn_{22}(Trz)_8(OH)_{12}$ - $(H_2O)_9 \cdot 8H_2O]_n$	70	12	99	24
$1_{0.1}$-$2_{0.4}$-$3_{0.5}$-JNM	25	3	99	25
Compound 1	60	12	98	26
1′@Ag NPs	25	4	99	27
Cu_2O@ZIF-8	40	6	99	28
Ag_{27}-MOF	26	6	97	29
Zn-MOF-2	50	12	93	30
MOF **1**	50	8	97	This work

^{1}H spectra for alkynyl carboxylic acids

3-phenylpropiolic acid (2a)

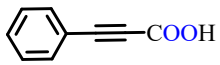

^{1}H NMR (600 MHz, $CDCl_3$) δ 7.62 (d, *J* = 6.8 Hz, 2H), 7.49 (d, *J* = 7.5 Hz, 1H), 7.39 (d, *J* = 7.7 Hz, 2H).

3-(*p*-tolyl)propiolic acid (2b)

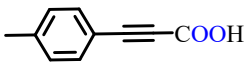

^{1}H NMR (600 MHz, $CDCl_3$) δ 7.51 (d, *J* = 8.1 Hz, 2H), 7.20 (d, *J* = 7.9 Hz, 2H), 2.39 (s, 3H).

3-(4-methoxyphenyl)propiolic acid (2c)

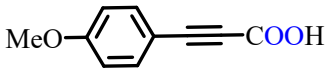

^{1}H NMR (600 MHz, $CDCl_3$) δ 7.57 (d, *J* = 8.8 Hz, 2H), 6.90 (d, *J* = 8.8 Hz, 2H), 3.85 (s, 3H).

3-(m-tolyl)propiolic acid (2d)

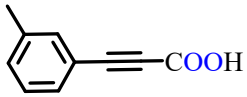

^{1}H NMR (600 MHz, CDCl3) δ 7.45 – 7.41 (m, 2H), 7.29 (s, 2H), 2.36 (s, 3H).

3-(3-methoxyphenyl)propiolic acid (2e)

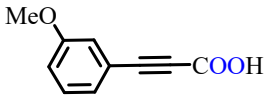

^{1}H NMR (600 MHz, $CDCl_3$) δ 7.30 (t, *J* = 7.9 Hz, 1H), 7.22 (d, *J* = 7.6 Hz, 1H), 7.12 (dd, *J* = 2.7, 1.4 Hz, 1H), 7.03 (dd, *J* = 8.4, 1.6 Hz, 1H), 3.82 (s, 3H).

3-(4-ethoxyphenyl)propiolic acid (2f)

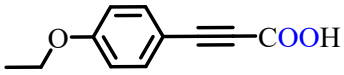

^{1}H NMR (600 MHz, DMSO) δ 7.56 (d, *J* = 8.8 Hz, 2H), 7.00 (d, *J* = 8.8 Hz, 2H), 4.09 (q, *J* = 7.0 Hz, 2H), 1.34 (t, *J* = 7.0 Hz, 3H).

3-(4-bromophenyl)propiolic acid (2g)

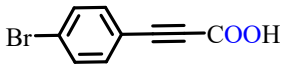

^{1}H NMR (600 MHz, DMSO) δ 7.68 (d, *J* = 8.5 Hz, 2H), 7.58 (d, *J* = 8.5 Hz, 2H).

3-(4-fluorophenyl)propiolic acid (2h)

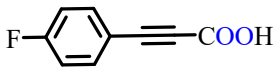

^{1}H NMR (600 MHz, $CDCl_3$) δ 7.64 – 7.60 (m, 2H), 7.10 (t, J = 8.5 Hz, 2H).

3-(4-cyanophenyl)propiolic acid (2i)

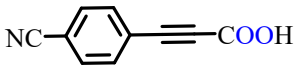

^{1}H NMR (600 MHz, DMSO) δ 7.95 (d, *J* = 8.4 Hz, 2H), 7.83 (d, *J* = 8.5 Hz, 2H).

3-(3-bromophenyl)propiolic acid (2j)

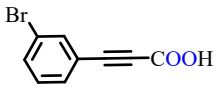

^{1}H NMR (600 MHz, $CDCl_3$) δ 7.76 (s, 1H), 7.62 (d, *J* = 8.1 Hz, 1H), 7.54 (d, *J* = 7.8 Hz, 1H), 7.28

(t, J = 8.0 Hz, 1H).

3-(3-fluorophenyl)propiolic acid (2k)

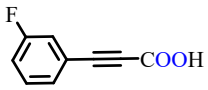

^{1}H NMR (600 MHz, $CDCl_3$) δ 7.42 – 7.28 (m, 3H), 7.23 – 7.17 (m, 1H).

4-phenoxybut-2-ynoic acid (2l)

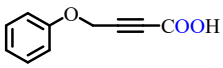

^{1}H NMR (600 MHz, $CDCl_3$) δ 7.34 – 7.31 (m, 2H), 7.04 (tt, J = 7.4, 1.1 Hz, 1H), 6.97 – 6.95 (m, 2H), 4.83 (s, 2H).

3-(thiophen-3-yl)propiolic acid (2m)

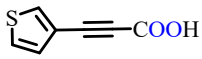

^{1}H NMR (600 MHz, DMSO) δ 8.17 (dd, J = 3.0, 1.2 Hz, 1H), 7.68 (dd, J = 5.0, 2.9 Hz, 1H), 7.31 (dd, J = 5.0, 1.2 Hz, 1H).

3-(naphthalen-2-yl)propiolic acid (2n)

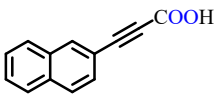

^{1}H NMR (600 MHz, DMSO) δ 8.29 (d, J = 1.6 Hz, 1H), 7.96 (ddd, J = 10.1, 7.5, 2.1 Hz, 3H), 7.61 – 7.56 (m, 3H).

3-(naphthalen-1-yl)propiolic acid (2o)

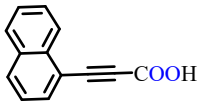

^{1}H NMR (600 MHz, $CDCl_3$) δ 11.06 (s, 1H), 8.35 (d, J = 8.4 Hz, 1H), 7.98 (d, J = 8.2 Hz, 1H), 7.91 – 7.87 (m, 2H), 7.65 (ddd, J = 8.3, 6.8, 1.3 Hz, 1H), 7.58 (ddd, J = 8.1, 6.8, 1.2 Hz, 1H), 7.48 (dd, J = 8.3, 7.1 Hz, 1H).

3-(3,5-dimethoxyphenyl)propiolic acid (2p)

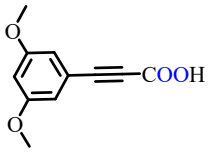

^{1}H NMR (600 MHz, DMSO) δ 6.76 (d, J = 2.3 Hz, 2H), 6.65 (t, J = 2.3 Hz, 1H), 3.76 (s, 6H).

3-(3,5-bis(trifluoromethyl)phenyl)propiolic acid (2q)

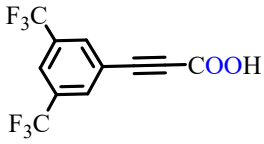

^{1}H NMR (600 MHz, DMSO) δ 8.31 (d, *J* = 1.7 Hz, 2H), 8.20 (s, 1H).

3,3'-(1,4-phenylene)dipropiolic acid (2r)

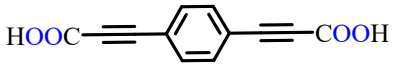

^{1}H NMR (600 MHz, DMSO) δ 7.71 (s, 4H).

3-([1,1'-biphenyl]-4-yl)propiolic acid (2s)

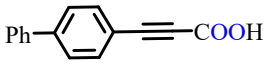

^{1}H NMR (600 MHz, DMSO) δ 7.81 – 7.69 (m, 6H), 7.50 (t, *J* = 7.7 Hz, 2H), 7.42 (t, *J* = 7.3 Hz, 1H).

but-2-ynoic acid (2t)

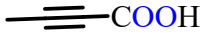

^{1}H NMR (600 MHz, DMSO) δ 1.99 (s, 3H).

oct-2-ynoic acid (2u)

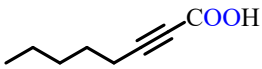

^{1}H NMR (600 MHz, $CDCl_3$) δ 10.77 (s, 1H), 2.33 (t, *J* = 7.2 Hz, 2H), 1.57 (p, *J* = 7.2 Hz, 2H), 1.40 – 1.29 (m, 4H), 0.89 (t, *J* = 7.2 Hz, 3H).

^{1}H spectra for cyclic carbonates

4-phenyl-1,3-dioxolan-2-one (4a)

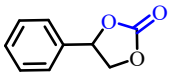

^{1}H NMR (600 MHz, $CDCl_3$) δ 7.48 – 7.30 (m, 5H), 5.67 (t, *J* = 8.0 Hz, 1H), 4.79 (t, *J* = 8.4 Hz, 1H), 4.35 – 4.31 (m, 1H).

4-ethyl-1,3-dioxolan-2-one (4b)

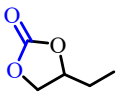

^{1}H NMR (600 MHz, $CDCl_3$) δ 4.55 (dt, J = 13.8, 7.0 Hz, 1H), 4.40 (dd, J = 8.6, 7.9 Hz, 1H), 3.95 (dd, J = 8.6, 6.9 Hz, 1H), 1.67 – 1.58 (m, 2H), 0.88 – 0.83 (m, 3H).

4-(chloromethyl)-1,3-dioxolan-2-one (4c)

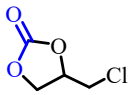

^{1}H NMR (600 MHz, $CDCl_3$) δ 5.01 – 4.92 (m, 1H), 4.58 (t, *J* = 8.6 Hz, 1H), 4.39 (dd, *J* = 8.9, 5.7 Hz, 1H), 3.80 – 3.70 (m, 2H).

4-(bromomethyl)-1,3-dioxolan-2-one (4d)

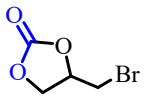

^{1}H NMR (600 MHz, $CDCl_3$) δ 4.97 – 4.88 (m, 1H), 4.51 (t, *J* = 8.4 Hz, 1H), 4.22 (dd, *J* = 8.9, 5.3 Hz, 1H), 3.61 – 3.48 (m, 2H).

4-butyl-1,3-dioxolan-2-one(4e)

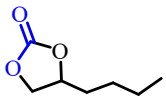

^{1}H NMR (600 MHz, $CDCl_3$) δ 4.68 – 4.61 (m, 1H), 4.46 (t, J = 8.2 Hz, 1H), 4.02 – 3.96 (m, 1H), 1.74 – 1.67 (m, 1H), 1.65 – 1.58 (m, 1H), 1.40 – 1.25 (m, 4H), 0.84 (t, J = 7.1 Hz, 3H).

4-(butoxymethyl)-1,3-dioxolan-2-one (4f)

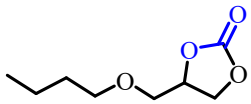

^{1}H NMR (600 MHz, $CDCl_3$) δ 4.74 (dt, *J* = 5.7, 2.8 Hz, 1H), 4.45 – 4.27 (m, 2H), 3.60 – 3.49 (m, 2H), 3.42 – 3.34 (m, 2H), 1.47 – 1.42 (m, 2H), 1.27 (q, *J* = 7.6 Hz, 2H), 0.82 (t, *J* = 7.3 Hz, 3H).

4-((neopentyloxy)methyl)-1,3-dioxolan-2-one (4g)

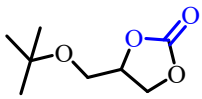

^{1}H NMR (600 MHz, $CDCl_3$) δ 4.76 – 4.68 (m, 1H), 4.41 (t, *J* = 8.3 Hz, 1H), 4.29 (dd, *J* = 8.3, 5.7 Hz, 1H), 3.55 (dd, *J* = 10.6, 3.9 Hz, 1H), 3.43 (dd, *J* = 10.6, 3.5 Hz, 1H), 1.11 (s, 9H).

4-((allyloxy)methyl)-1,3-dioxolan-2-one (4h)

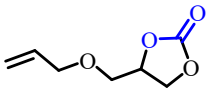

^{1}H NMR (600 MHz, $CDCl_3$) δ 5.88 – 5.80 (m, 1H), 5.25 (dd, *J* = 17.3, 1.7 Hz, 1H), 5.19 (dd, *J* = 10.4, 1.5 Hz, 1H), 4.84 – 4.78 (m, 1H), 4.48 (t, *J* = 8.4 Hz, 1H), 4.37 (dd, *J* = 8.4, 6.0 Hz, 1H), 4.03

(t, *J* = 5.2 Hz, 2H), 3.67 (dd, *J* = 11.1, 3.8 Hz, 1H), 3.59 (dd, *J* = 11.1, 3.7 Hz, 1H).

4-((benzyloxy)methyl)-1,3-dioxolan-2-one (4i)

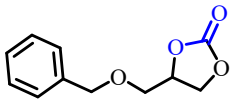

^{1}H NMR (600 MHz, $CDCl_3$) δ 7.28 – 7.21 (m, 5H), 4.72 – 4.65 (m, 1H), 4.47 (q, *J* = 12.1 Hz, 2H), 4.33 (t, *J* = 8.5 Hz, 1H), 4.24 (dd, *J* = 8.4, 5.9 Hz, 1H), 3.60 (dd, *J* = 11.2, 3.4 Hz, 1H), 3.48 (dd, *J* = 11.1, 3.7 Hz, 1H).

4-((benzyloxy)methyl)-1,3-dioxolan-2-one (4j)

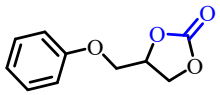

^{1}H NMR (600 MHz, $CDCl_3$) δ7.30 (t, J = 7.7 Hz, 2H), 7.01 (t, J = 7.3 Hz, 1H), 6.91 (dt, J = 7.7, 1.0 Hz, 2H), 5.02 (dq, J = 8.9, 3.9 Hz, 1H), 4.60 (t, J = 8.5 Hz, 1H), 4.52 (dd, J = 8.5, 5.9 Hz, 1H), 4.23 (dd, J = 10.6, 4.1 Hz, 1H), 4.13 (dd, J = 10.6, 3.6 Hz, 1H).

tetrahydro-4H-cyclopenta[d][1,3]dioxol-2-one (4k)

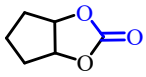

^{1}H NMR (600 MHz, $CDCl_3$) δ 5.07 – 5.02 (m, 2H), 2.09 (dd, *J* = 14.2, 5.1 Hz, 2H), 1.77 – 1.67 (m, 2H), 1.66 – 1.57 (m, 2H).

hexahydrobenzo[d][1,3]dioxol-2-one (4l)

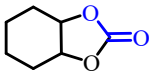

^{1}H NMR (600 MHz, $CDCl_3$) δ 4.64 (t, *J* = 4.2 Hz, 2H), 1.88 – 1.76 (m, 4H), 1.57 – 1.49 (m, 2H), 1.40 – 1.33 (m, 2H).

^{1}H spectra for oxazolidinones

3-Benzyl-5-methyleneoxazolidin-2-one (6a)

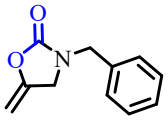

^{1}H NMR (600 MHz, $CDCl_3$) δ 7.39 – 7.26 (m, 5H), 4.74 (q, *J* = 2.8 Hz, 1H), 4.47 (s, 2H), 4.24 (q, *J* = 2.5 Hz, 1H), 4.02 (t, *J* = 2.4 Hz, 2H).

3-(4-fluorobenzyl)-5 methyleneoxazolidin-2-one1 (6b)

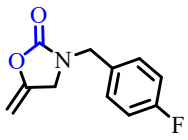

^{1}H NMR (600 MHz, $CDCl_3$) δ 7.25 – 7.19 (m, 2H), 7.00 (t, *J* = 8.6 Hz, 2H), 4.67 (q, *J* = 2.8 Hz, 1H), 4.39 (s, 2H), 4.22 (dd, *J* = 3.6, 1.8 Hz, 1H), 3.99 (t, *J* = 2.5 Hz, 2H).

3-(4-chlorphenyl)-5-methyleneoxazolidin-2-one (6c)

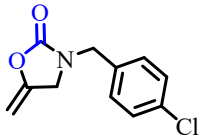

^{1}H NMR (600 MHz, $CDCl_3$) δ 7.25 (s, 2H), 7.15 (d, *J* = 8.1 Hz, 2H), 4.66 (q, *J* = 2.9 Hz, 1H), 4.36 (s, 2H), 4.19 (q, *J* = 2.6 Hz, 1H), 3.96 (t, *J* = 2.5 Hz, 2H).

3-(4-bromobenzyl)-5-methyleneoxazolidin-2-one (6d)

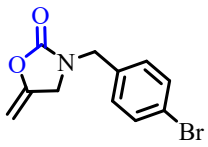

^{1}H NMR (600 MHz, $CDCl_3$) δ 7.29 – 7.25 (m, 2H), 6.98 – 6.94 (m, 2H), 4.52 (q, *J* = 2.8 Hz, 1H), 4.21 (s, 2H), 4.06 (dt, *J* = 3.2, 2.2 Hz, 1H), 3.83 (t, *J* = 2.5 Hz, 2H).

3-(4-methylbenzyl)-5 methyleneoxazolidin-2-one (6e)

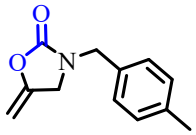

^{1}H NMR (600 MHz, $CDCl_3$) δ 7.37 – 7.21 (m, 4H), 4.82 (q, *J* = 2.9 Hz, 1H), 4.52 (s, 2H), 4.32 (q, *J* = 2.6 Hz, 1H), 4.10 (t, *J* = 2.4 Hz, 2H), 2.44 (s, 3H).

3-(3-methylbenzyl)-5-methyleneoxazolidin-2-one (6f)

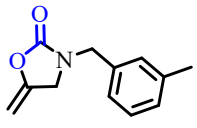

^{1}H NMR (600 MHz, $CDCl_3$) δ 7.23 (t, *J* = 7.6 Hz, 1H), 7.12 (d, *J* = 7.6 Hz, 1H), 7.09 – 7.04 (m, 2H), 4.71 (q, *J* = 2.8 Hz, 1H), 4.41 (s, 2H), 4.23 (dt, *J* = 3.1, 2.2 Hz, 1H), 4.01 (t, *J* = 2.4 Hz, 2H), 2.34 (s, 3H).

3-(4-methoxybenzyl)-5-methyleneoxazolidin-2-one (6g)

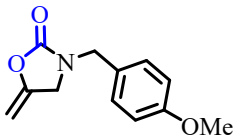

^{1}H NMR (600 MHz, $CDCl_3$) δ 7.19 (d, *J* = 8.6 Hz, 2H), 6.88 (d, *J* = 8.6 Hz, 2H), 4.71 (q, *J* = 2.8 Hz, 1H), 4.39 (s, 2H), 4.22 (dt, *J* = 3.2, 2.2 Hz, 1H), 3.99 (t, *J* = 2.4 Hz, 2H), 3.80 (s, 3H).

5-methylene-3-(4-(trifluoromethyl)benzyl)oxazolidin-2-one (6h)

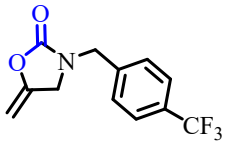

^{1}H NMR (600 MHz, $CDCl_3$) δ 7.46 (d, *J* = 8.1 Hz, 2H), 7.27 (s, 2H), 4.57 (q, *J* = 2.8 Hz, 1H), 4.38 (s, 2H), 4.15 – 4.10 (m, 1H), 3.93 (t, *J* = 2.5 Hz, 2H).

4-((5-methylene-2-oxooxazolidin-3-yl)methyl)benzonitrile (6i)

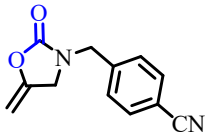

^{1}H NMR (600 MHz, $CDCl_3$) δ 7.60 – 7.56 (m, 2H), 7.36 – 7.33 (m, 2H), 4.65 (q, *J* = 2.8 Hz, 1H), 4.46 (s, 2H), 4.22 (q, *J* = 2.4 Hz, 1H), 4.03 (t, *J* = 2.5 Hz, 2H).

3-(2,4-difluorobenzyl)-5-methyleneoxazolidin-2-one (6j)

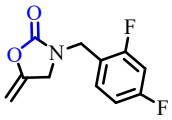

^{1}H NMR (600 MHz, $CDCl_3$) δ 7.31 (td, *J* = 8.5, 6.3 Hz, 1H), 6.87 – 6.76 (m, 2H), 4.68 (q, *J* = 2.8 Hz, 1H), 4.45 (d, *J* = 1.5 Hz, 2H), 4.23 (dt, *J* = 3.2, 2.2 Hz, 1H), 4.07 (t, *J* = 2.5 Hz, 2H).

3-(3,4-dichlorobenzyl)-5-methyleneoxazolidin-2-one (6k)

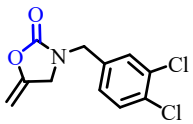

^{1}H NMR (600 MHz, $CDCl_3$) δ 7.40 – 7.30 (m, 2H), 7.09 (dd, *J* = 8.2, 2.1 Hz, 1H), 4.68 (q, *J* = 2.7 Hz, 1H), 4.36 (s, 2H), 4.24 (dt, *J* = 3.3, 2.2 Hz, 1H), 4.02 (t, *J* = 2.4 Hz, 2H).

3-(1-Phenethyl)-5-methyleneoxazolidin-2-one (6l)

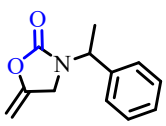

^{1}H NMR (600 MHz, $CDCl_3$) δ 7.46 – 7.08 (m, 5H), 5.15 (q, *J* = 7.1 Hz, 1H), 4.60 (q, *J* = 2.8 Hz, 1H), 4.13 (dd, *J* = 3.1, 2.0 Hz, 1H), 4.02 (dt, *J* = 14.3, 2.4 Hz, 1H), 3.71 – 3.65 (m, 1H), 1.50 (d, *J* = 7.2 Hz, 3H).

3-Phenethyl-5-methyleneoxazolidin-2-one (6m)

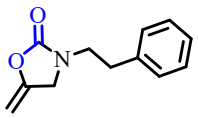

^{1}H NMR (600 MHz, $CDCl_3$) δ 7.32 – 7.01 (m, 5H), 4.62 (d, *J* = 2.8 Hz, 1H), 4.15 (d, *J* = 3.1 Hz, 1H), 3.93 (t, *J* = 2.4 Hz, 2H), 3.51 – 3.47 (m, 2H), 2.82 (t, *J* = 7.3 Hz, 2H).

5-methylene-3-(pyridin-2-ylmethyl)oxazolidin-2-one (6n)

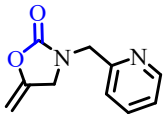

^{1}H NMR (600 MHz, $CDCl_3$) δ 8.56 (d, *J* = 4.9 Hz, 1H), 7.70 (td, *J* = 7.7, 1.8 Hz, 1H), 7.31 (d, *J* = 7.8 Hz, 1H), 7.25 – 7.22 (m, 1H), 4.75 (q, *J* = 2.8 Hz, 1H), 4.58 (s, 2H), 4.27 – 4.26 (m, 1H), 4.23 (t, *J* = 2.4 Hz, 2H).

3-(furan-2-ylmethyl)-5-methyleneoxazolidin-2-one (6o)

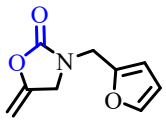

^{1}H NMR (600 MHz, $CDCl_3$) δ 7.34 (dd, *J* = 1.9, 0.9 Hz, 1H), 6.31 – 6.26 (m, 2H), 4.67 (q, *J* = 2.8 Hz, 1H), 4.41 (s, 2H), 4.24 – 4.22 (m, 1H), 4.09 (t, *J* = 2.4 Hz, 2H).

5-methylene-3-(thiophen-2-ylmethyl)oxazolidin-2-one (6p)

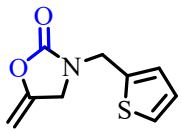

^{1}H NMR (600 MHz, $CDCl_3$) δ 7.22 – 7.16 (m, 1H), 6.96 – 6.86 (m, 2H), 4.64 (d, *J* = 2.9 Hz, 1H), 4.56 (s, 2H), 4.18 (d, *J* = 2.8 Hz, 1H), 4.02 (t, *J* = 2.5 Hz, 2H).

3-(2-(1H-indol-3-yl)ethyl)-5-methyleneoxazolidin-2-one (6q)

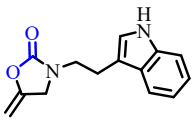

^{1}H NMR (600 MHz, $CDCl_3$) δ 8.31 (s, 1H), 7.60 (dd, *J* = 7.9, 1.2 Hz, 1H), 7.38 (dt, *J* = 8.1, 0.9 Hz, 1H), 7.22 (t, *J* = 7.0 Hz, 1H), 7.15 (d, *J* = 8.0 Hz, 1H), 7.03 (s, 1H), 4.70 (q, *J* = 2.8 Hz, 1H), 4.19

(q, *J* = 2.3 Hz, 1H), 4.02 (t, *J* = 2.4 Hz, 2H), 3.65 (t, *J* = 7.2 Hz, 2H), 3.05 (t, *J* = 7.2 Hz, 2H).

3-Cyclohexyl-5-methyleneoxazolidin-2-one (6r)

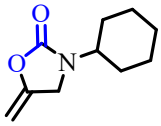

^{1}H NMR (600 MHz, $CDCl_3$) δ 4.65 (t, *J* = 2.7 Hz, 1H), 4.23 (q, *J* = 2.6 Hz, 1H), 4.09 (d, *J* = 2.5 Hz, 2H), 3.66 (m, 1H), 1.79 – 1.74 (m, 4H), 1.64 – 1.60 (d, 1H), 1.30 (m, 4H), 1.09 – 1.01 (m, 1H).

3-cyclopentyl-5-methyleneoxazolidin-2-one (6s)

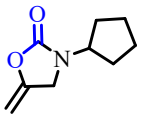

^{1}H NMR (600 MHz, $CDCl_3$) δ 4.53 (q, *J* = 2.7 Hz, 1H), 4.16 – 4.14 (m, 1H), 4.07 (p, *J* = 8.0 Hz, 1H), 4.02 (t, *J* = 2.5 Hz, 2H), 1.78 – 1.71 (m, 2H), 1.57 (d, *J* = 3.1 Hz, 2H), 1.49 – 1.39 (m, 4H).

3-methyl-5-methyleneoxazolidin-2-one (6t)

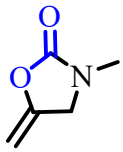

^{1}H NMR (600 MHz, $CDCl_3$) δ 4.65 (q, *J* = 2.8 Hz, 1H), 4.24 – 4.22 (m, 1H), 4.12 (t, *J* = 2.4 Hz, 2H), 2.86 (s, 3H).

4,4-dimethyl-5-methyleneoxazolidin-2-one **(6u)**

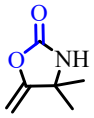

^{1}H NMR (600 MHz, $CDCl_3$) δ 7.06 (s, 1H), 4.59 (dd, J = 3.4, 1.1 Hz, 1H), 4.19 (d, J = 3.4 Hz, 1H), 1.42 (s, 6H).

3-(5-methylene-2-oxooxazolidin-3-yl)propanenitrile (6v)

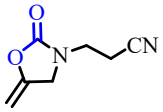

^{1}H NMR (600 MHz, $CDCl_3$) δ 4.79 (q, *J* = 2.8 Hz, 1H), 4.35 (d, *J* = 2.7 Hz, 3H), 3.60 (t, *J* = 6.4 Hz, 2H), 2.67 (t, *J* = 6.4 Hz, 2H).

3-(2-methoxyethyl)-5-methyleneoxazolidin-2-one (6w)

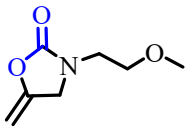

^{1}H NMR (600 MHz, $CDCl_3$) δ 4.72 (q, *J* = 2.7 Hz, 1H), 4.28 (t, *J* = 2.4 Hz, 2H), 4.27 – 4.25 (m, 1H), 3.56 – 3.53 (m, 2H), 3.48 – 3.45 (m, 2H), 3.34 (s, 3H).

3-dodecyl-5-methyleneoxazolidin-2-one (6x)

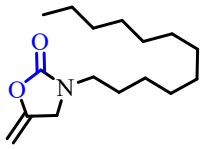

^{1}H NMR (600 MHz, $CDCl_3$) δ 4.72 (q, *J* = 2.7 Hz, 1H), 4.27 (dt, *J* = 3.1, 2.2 Hz, 1H), 4.14 (t, *J* = 2.4 Hz, 2H), 3.29 – 3.26 (m, 2H), 1.53 (q, *J* = 7.2 Hz, 2H), 1.27 (d, *J* = 29.1 Hz, 18H), 0.87 (t, *J* = 7.0 Hz, 3H).

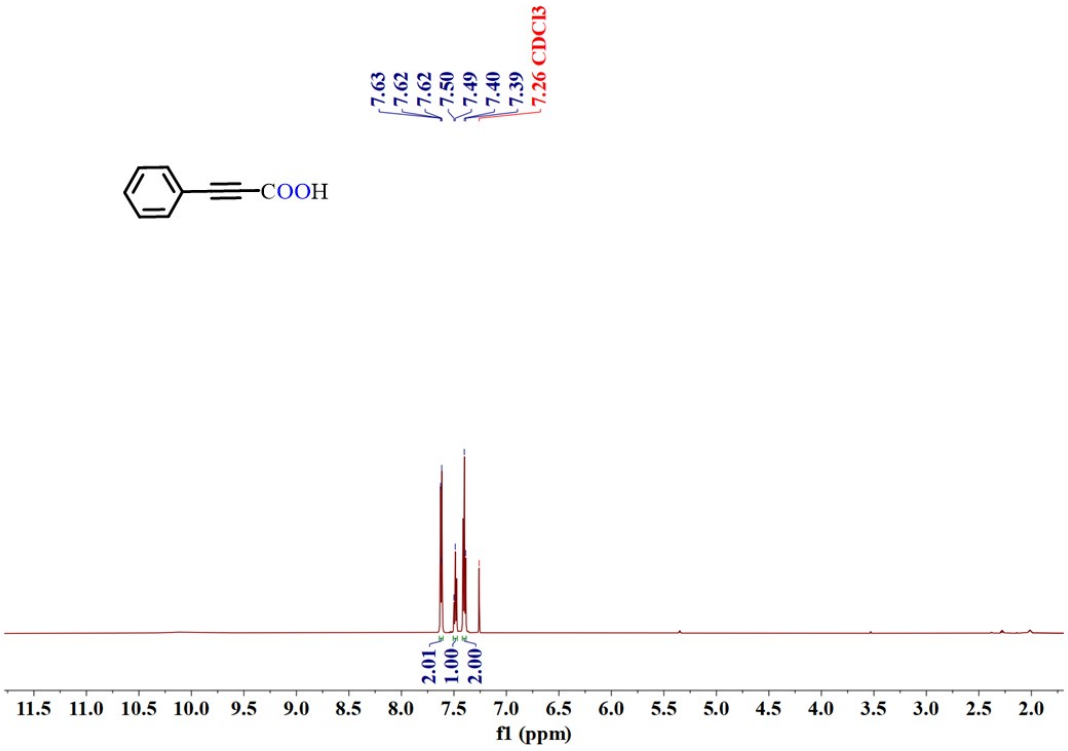

^{1}H NMR (600 MHz, $CDCl_3$) spectrum of 2a

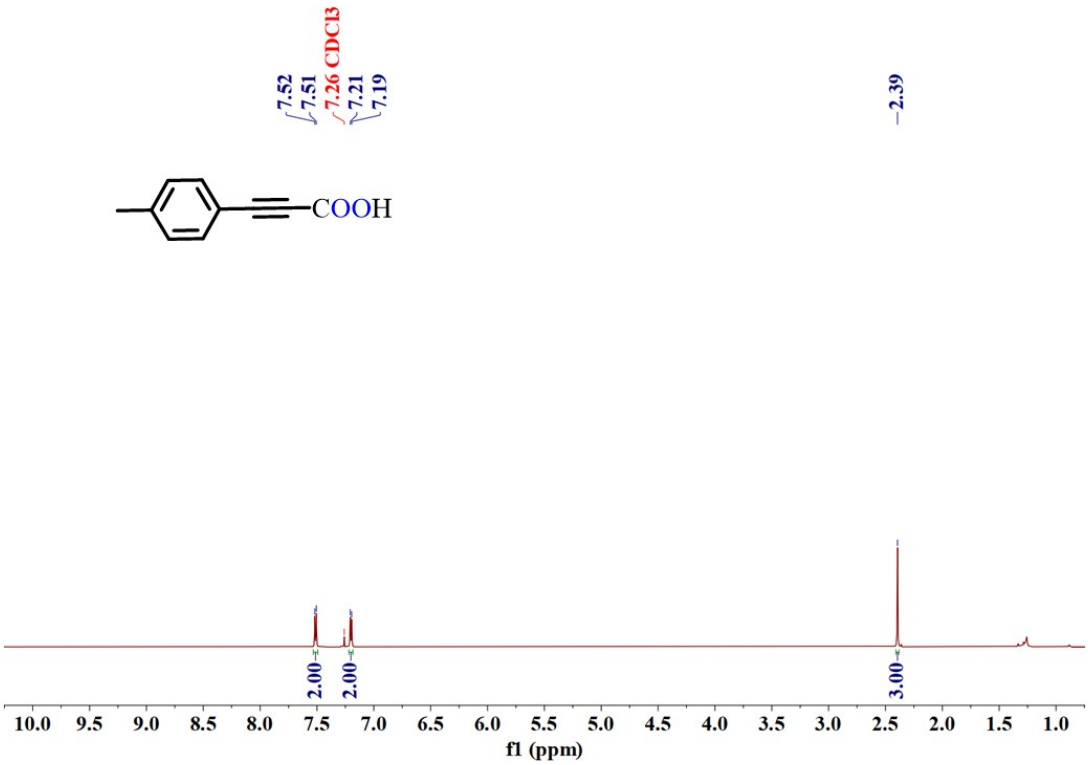

^{1}H NMR (600 MHz, $CDCl_3$) spectrum of 2b

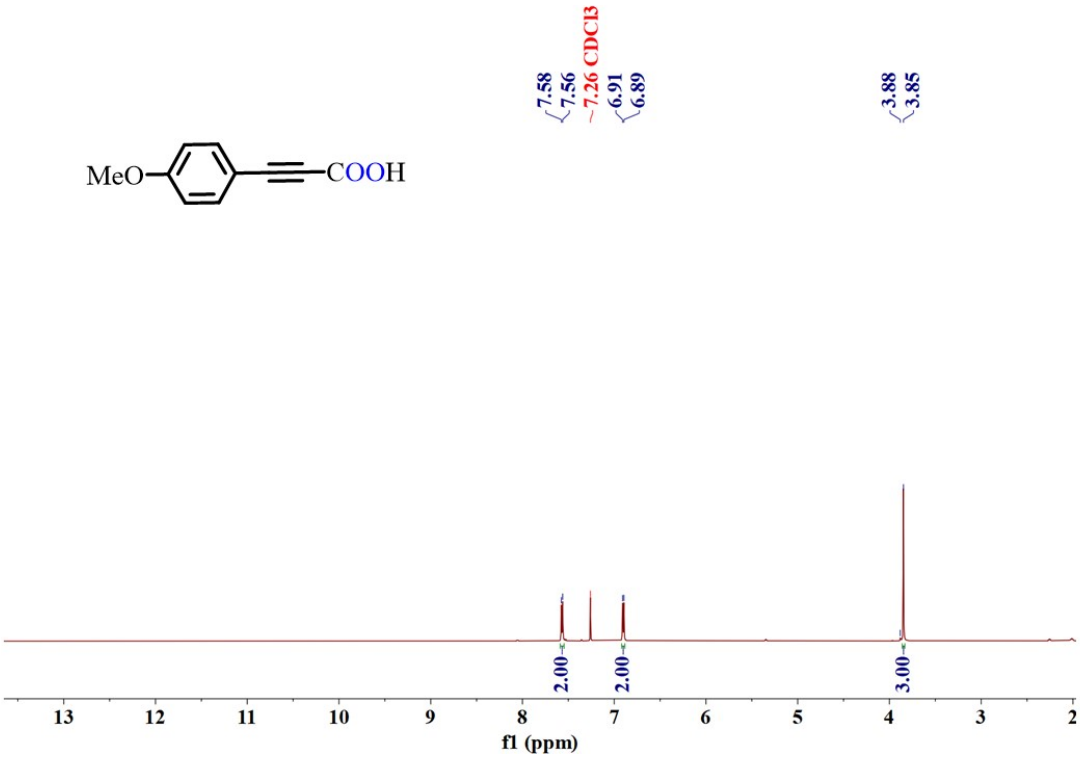

^{1}H NMR (600 MHz, $CDCl_3$) spectrum of 2c

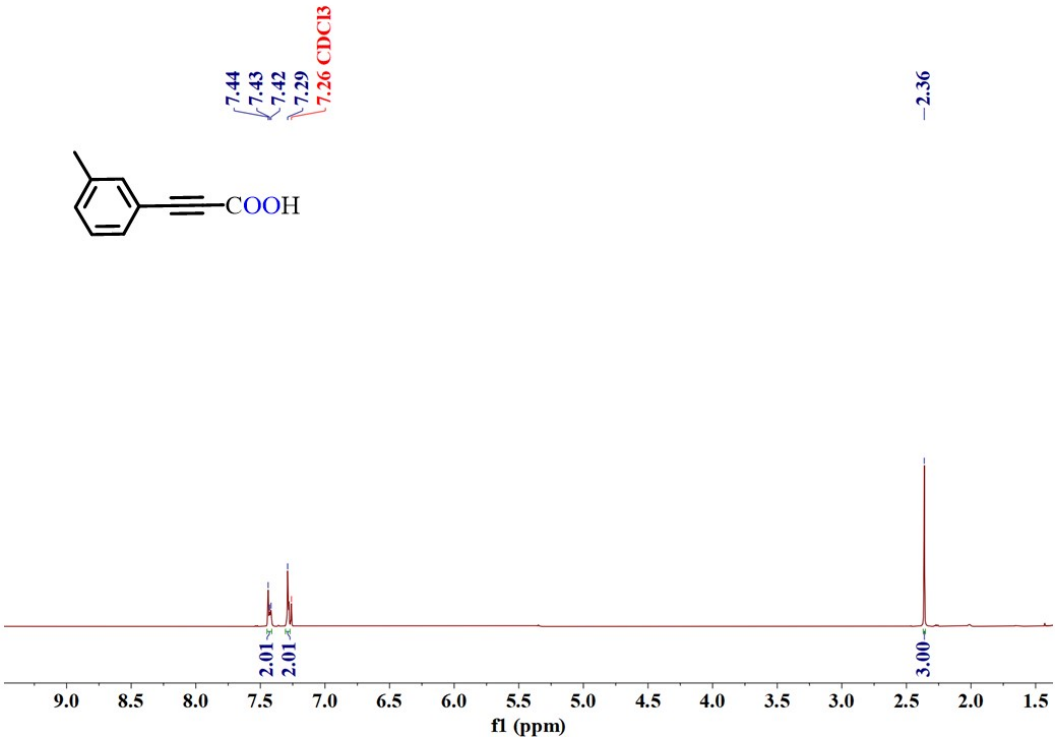

^{1}H NMR (600 MHz, $CDCl_3$) spectrum of 2d

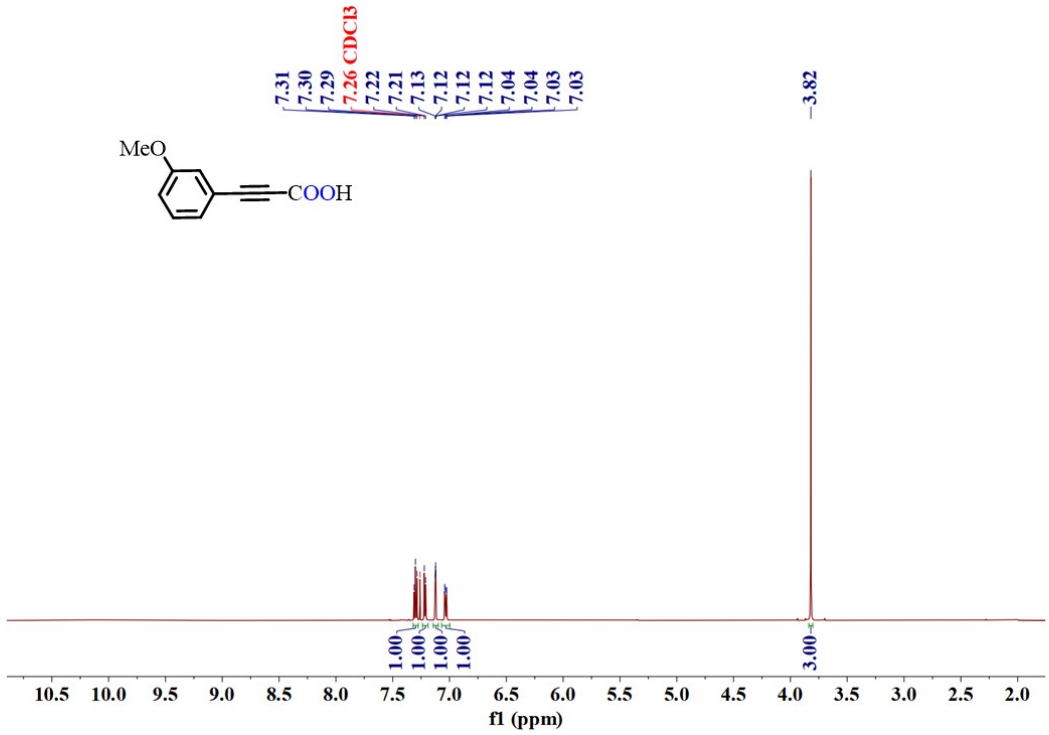

^{1}H NMR (600 MHz, $CDCl_3$) spectrum of 2e

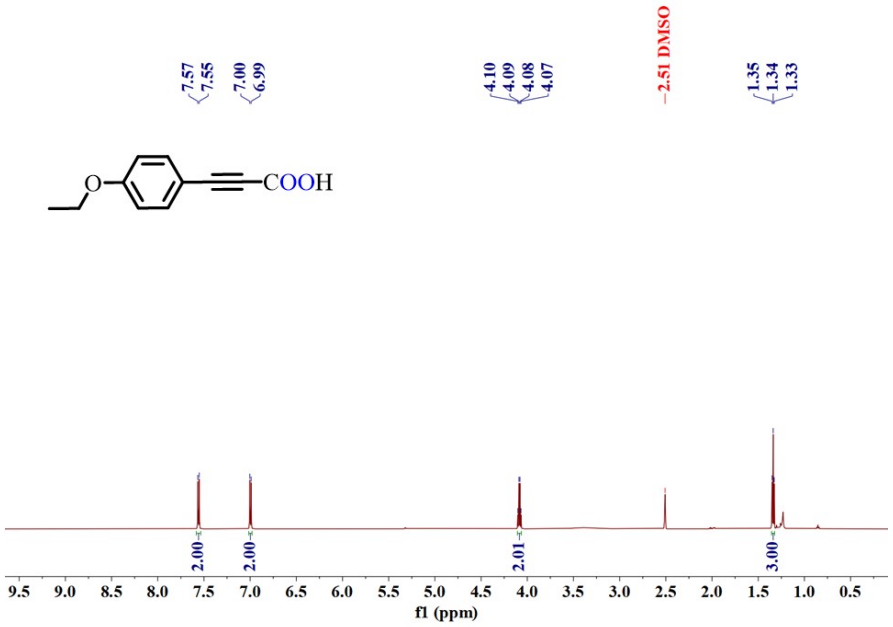

^{1}H NMR (600 MHz, $CDCl_3$) spectrum of 2f

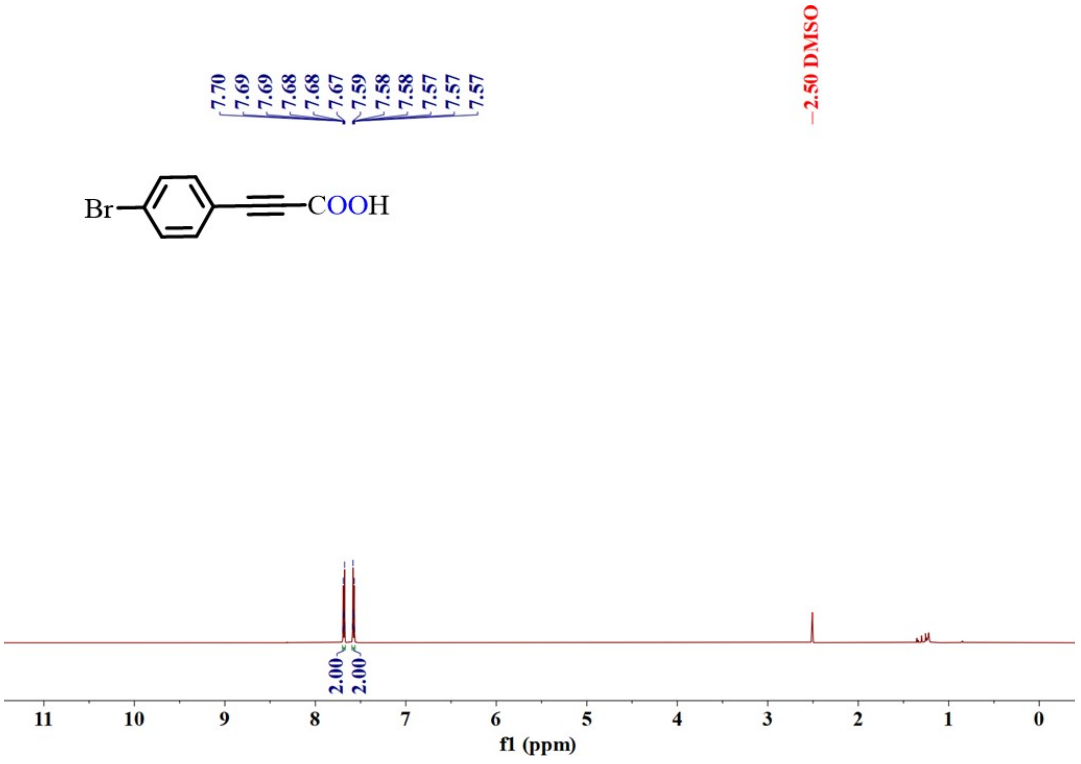

^{1}H NMR (600 MHz, $CDCl_3$) spectrum of 2g

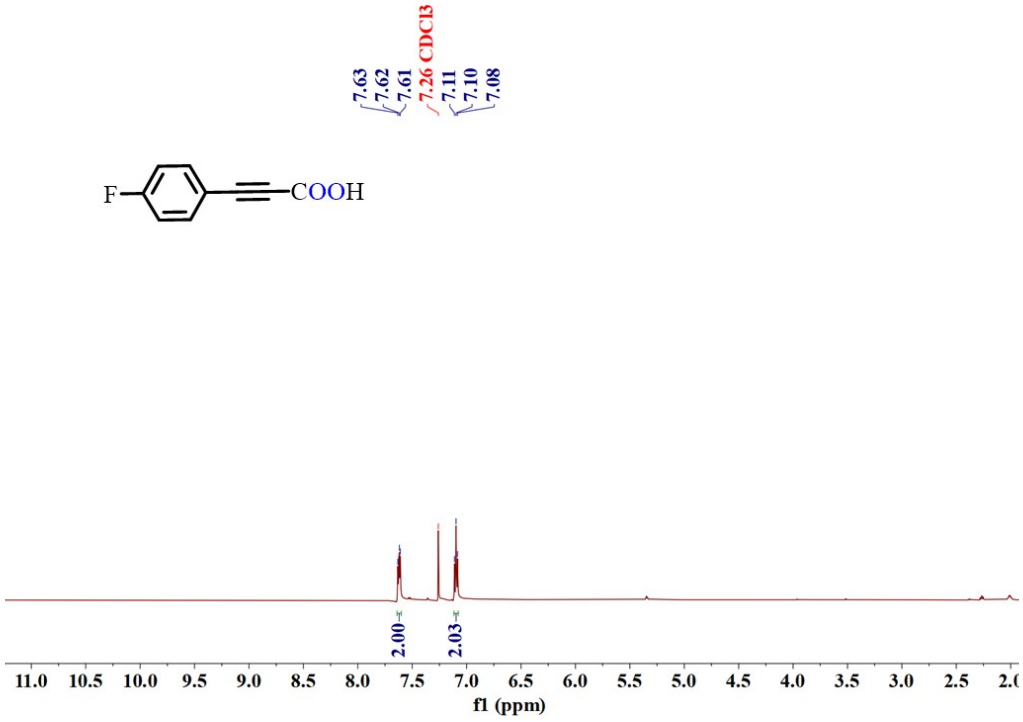

^{1}H NMR (600 MHz, $CDCl_3$) spectrum of 2h

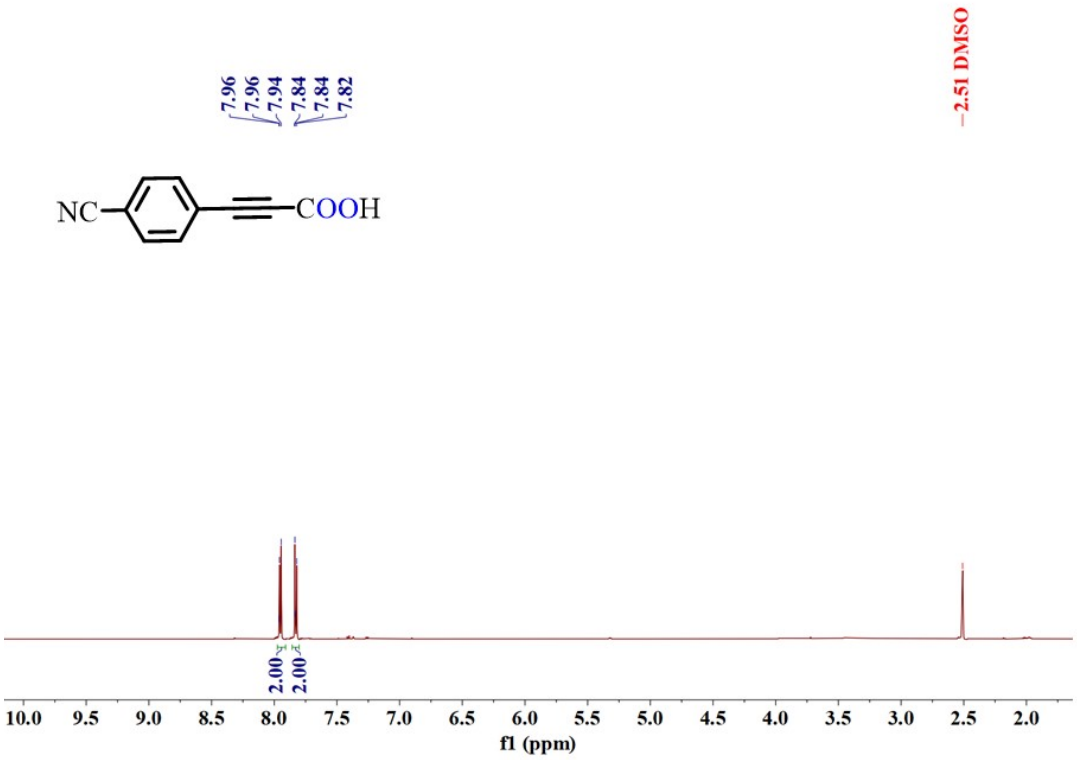

^{1}H NMR (600 MHz, $CDCl_3$) spectrum of 2i

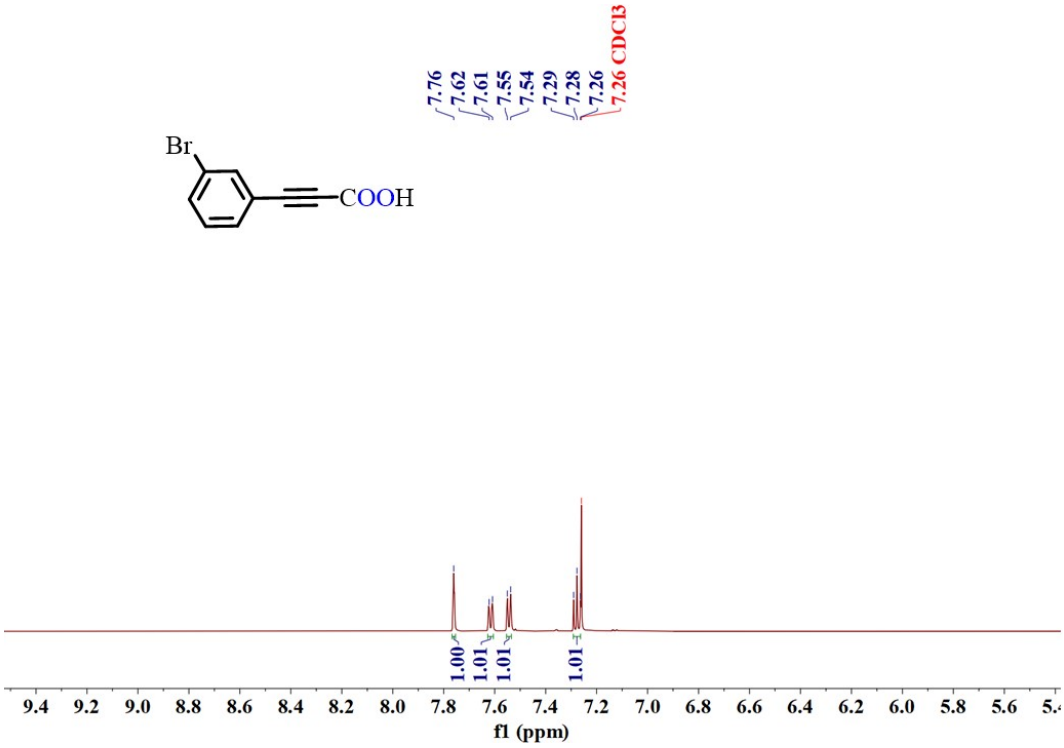

^{1}H NMR (600 MHz, $CDCl_3$) spectrum of 2j

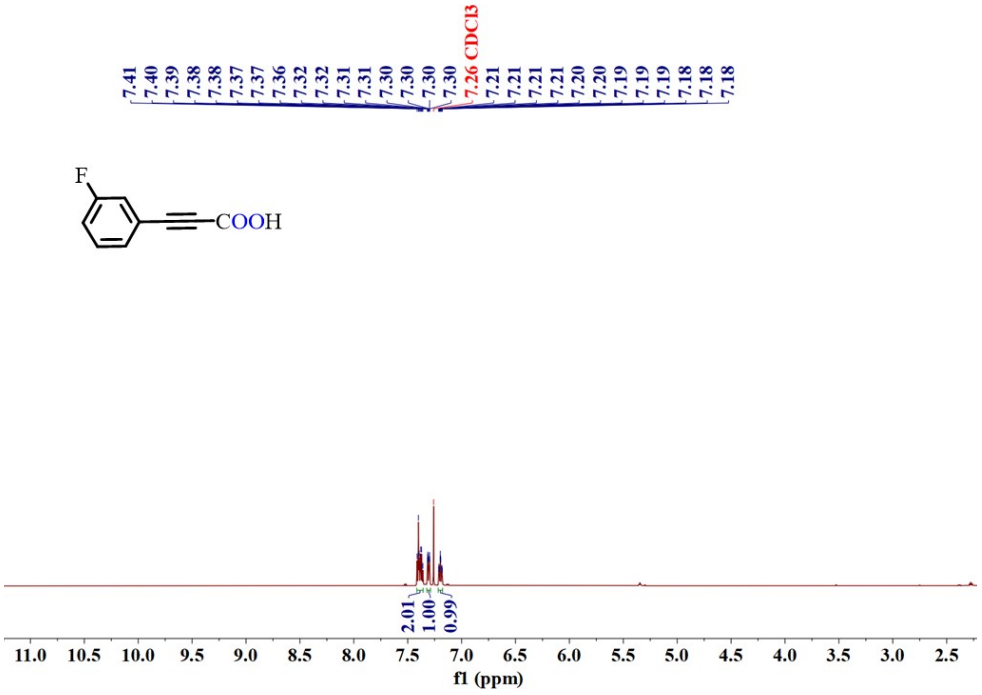

^{1}H NMR (600 MHz, $CDCl_3$) spectrum of 2k

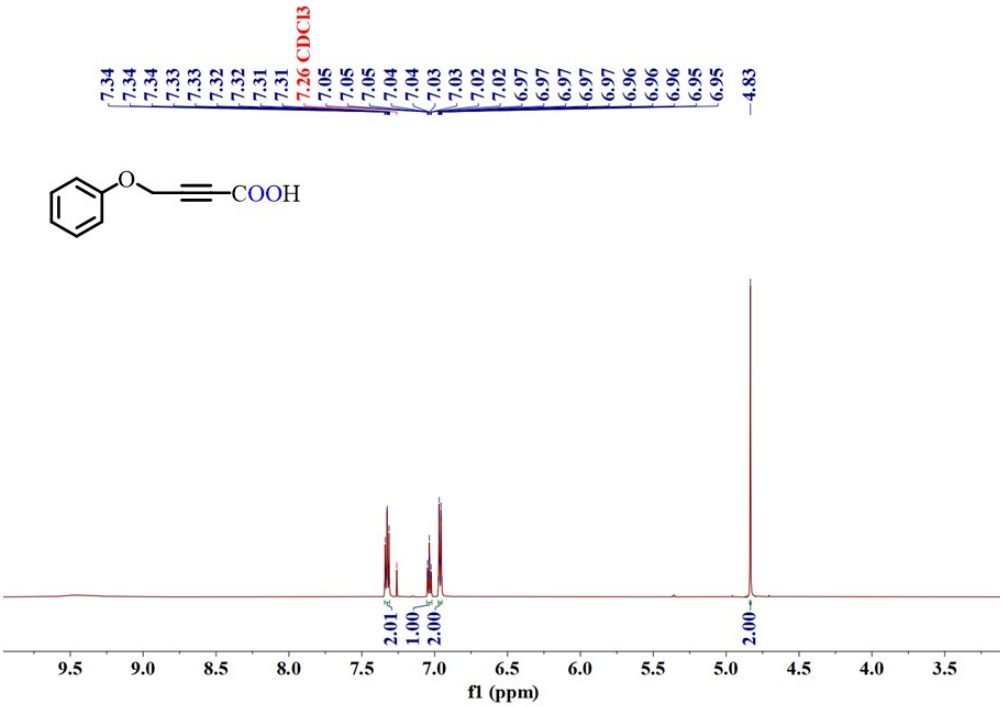

^{1}H NMR (600 MHz, $CDCl_3$) spectrum of 2l

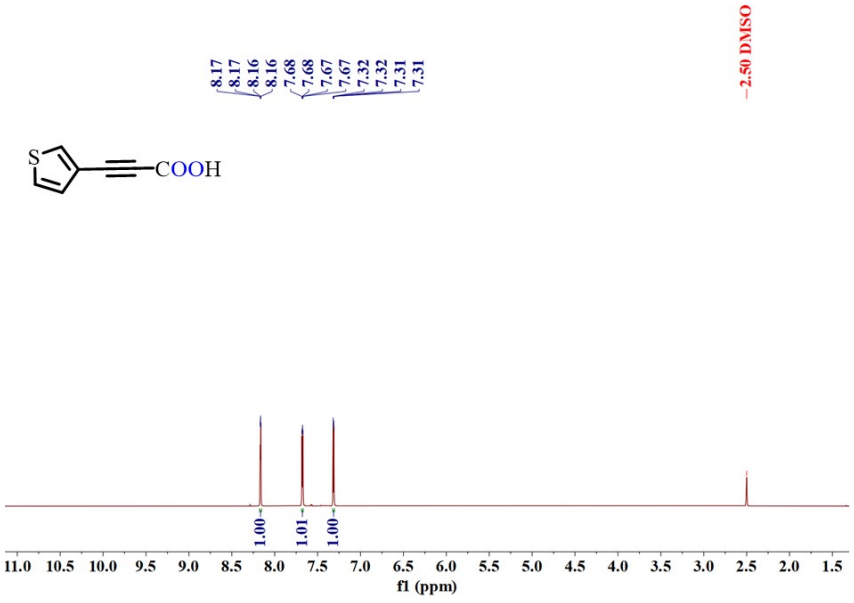

^{1}H NMR (600 MHz, $CDCl_3$) spectrum of 2m

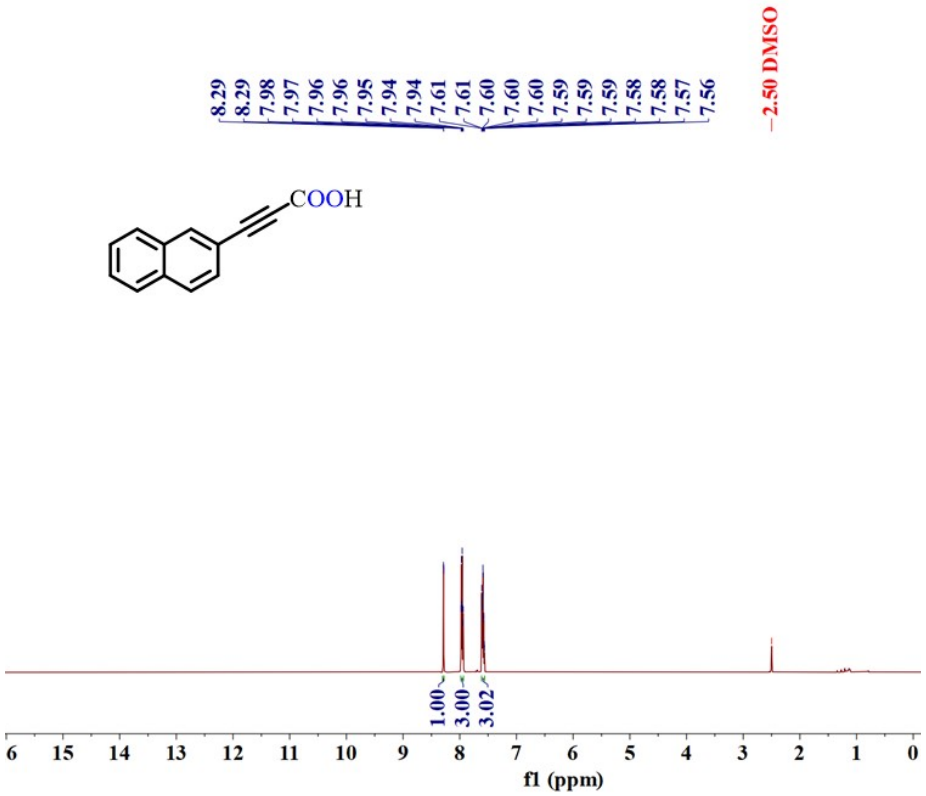

^{1}H NMR (600 MHz, $CDCl_3$) spectrum of 2n

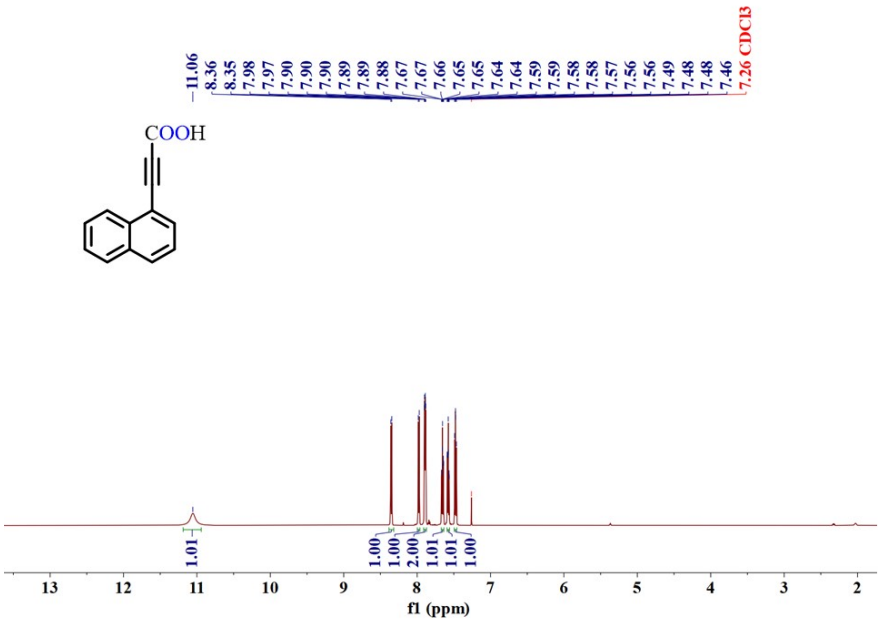

^{1}H NMR (600 MHz, $CDCl_3$) spectrum of 2o

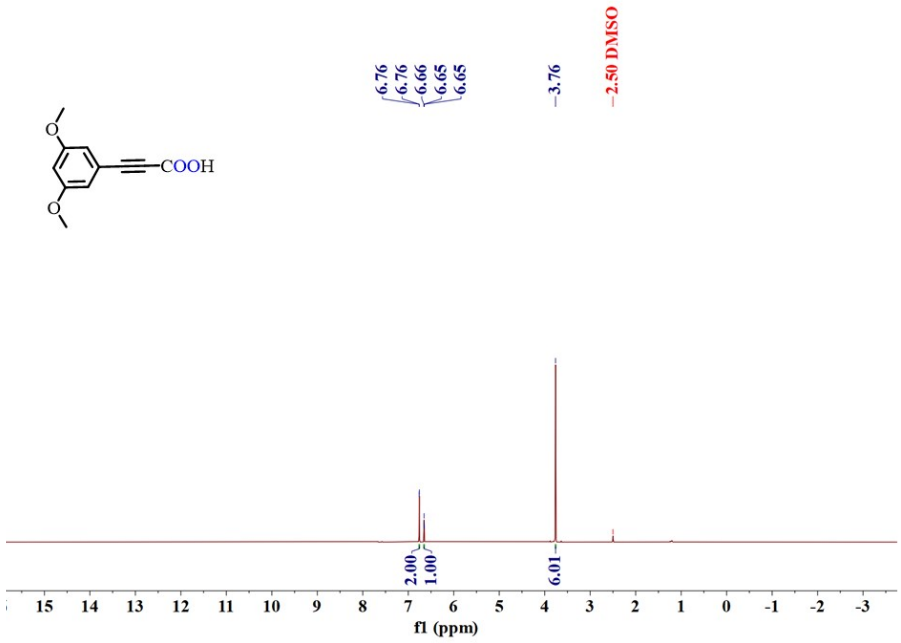

^{1}H NMR (600 MHz, $CDCl_3$) spectrum of 2p

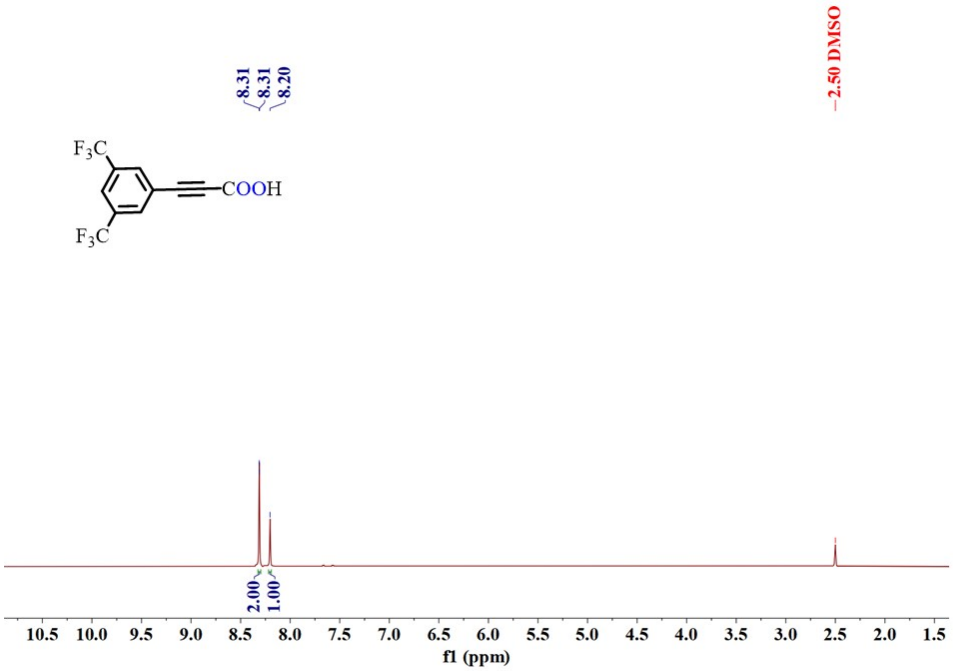

^{1}H NMR (600 MHz, $CDCl_3$) spectrum of 2q

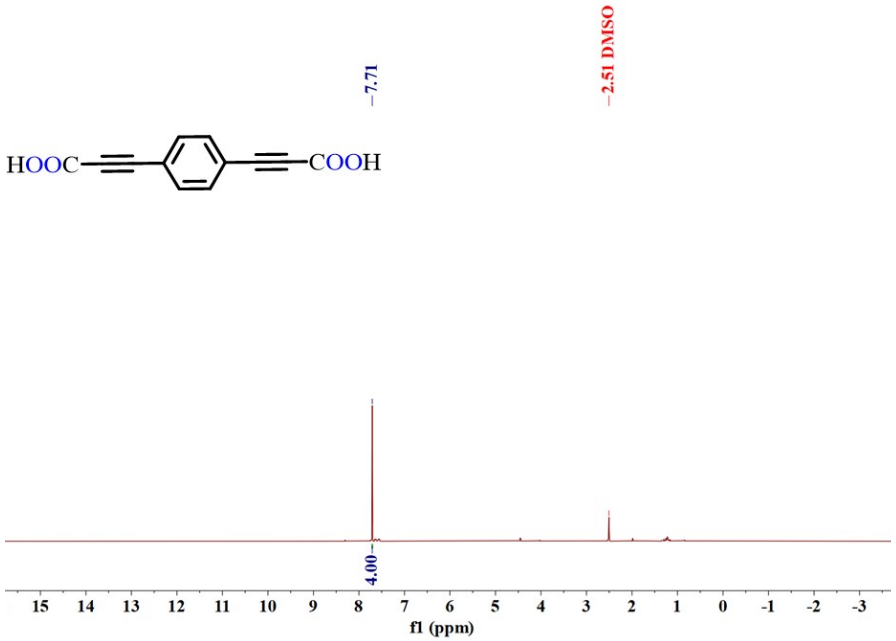

^{1}H NMR (600 MHz, $CDCl_3$) spectrum of 2r

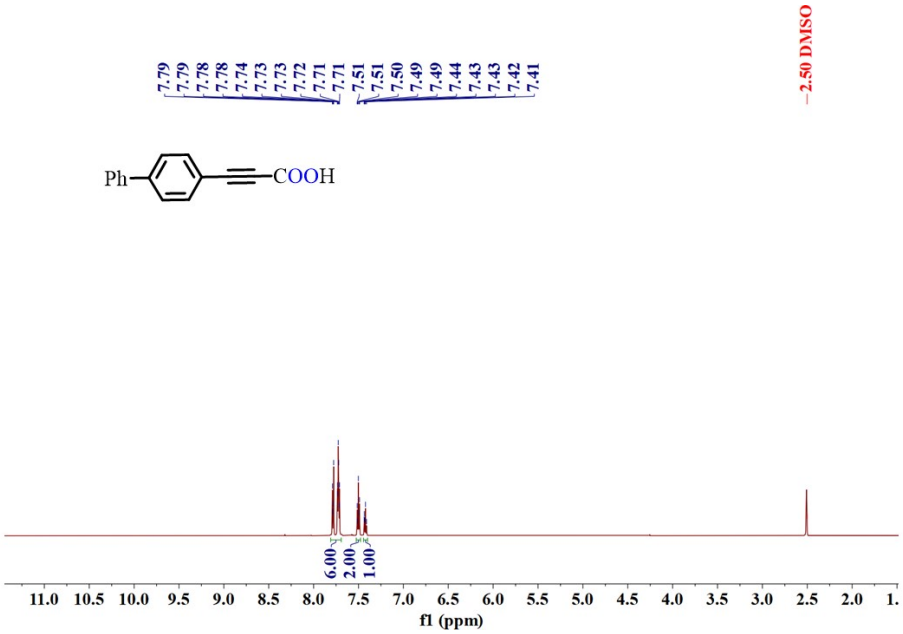

^{1}H NMR (600 MHz, $CDCl_3$) spectrum of 2s

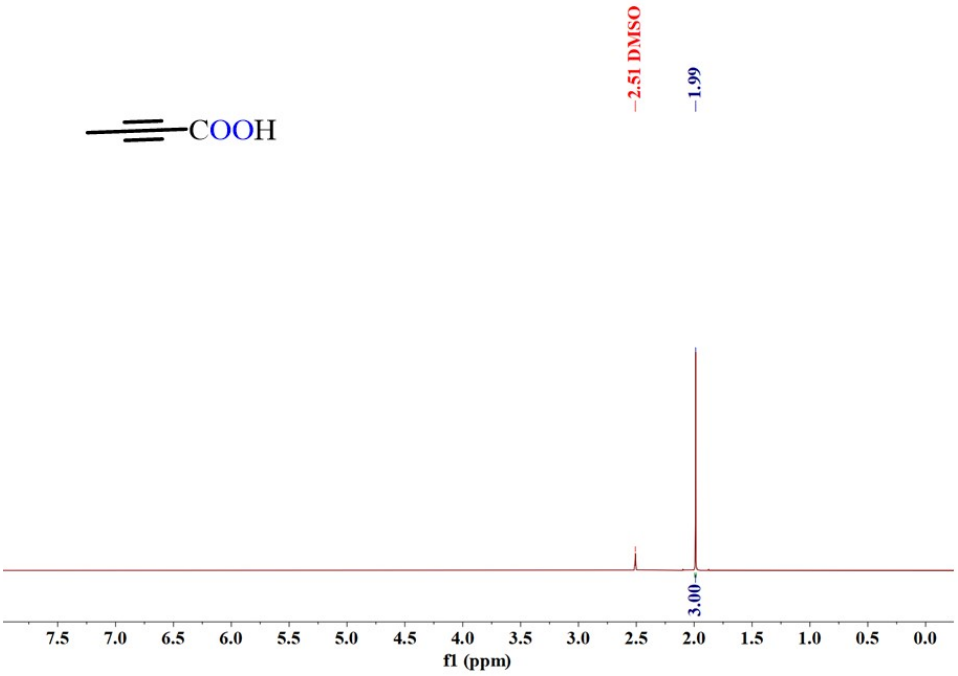

^{1}H NMR (600 MHz, $CDCl_3$) spectrum of 2t

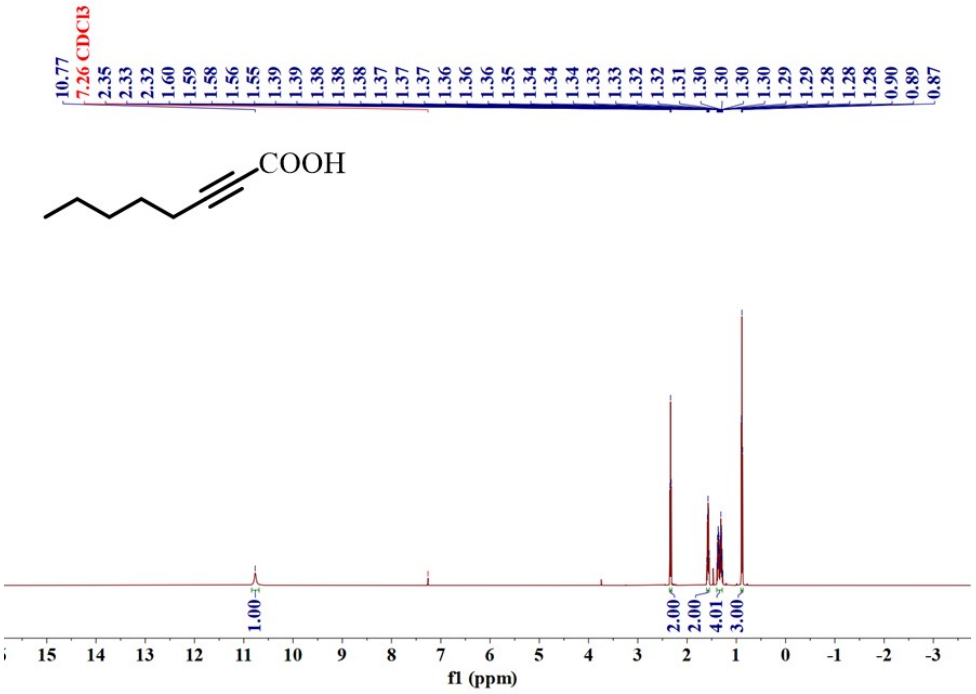

^{1}H NMR (600 MHz, $CDCl_3$) spectrum of 2u

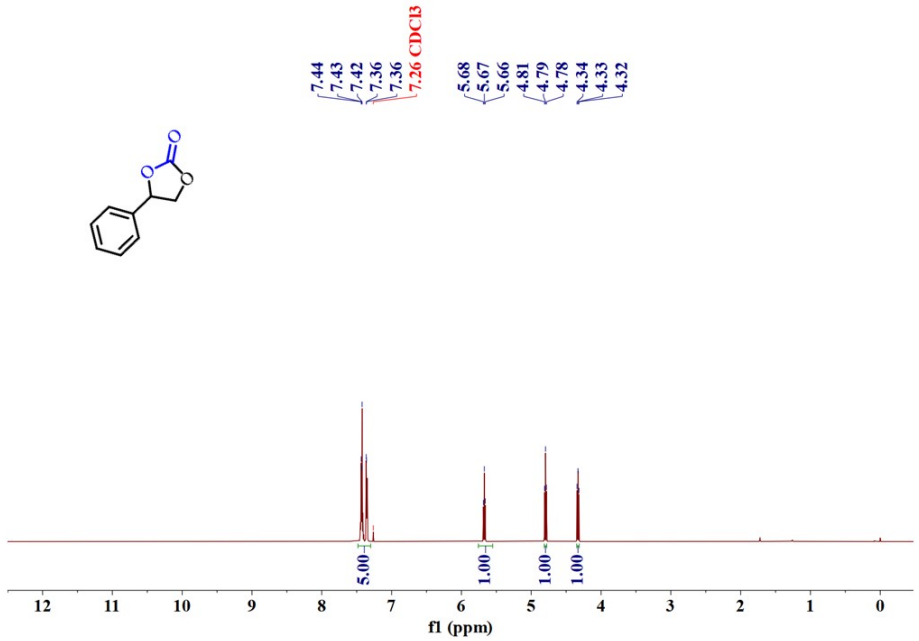

^{1}H NMR (600 MHz, $CDCl_3$) spectrum of 4a

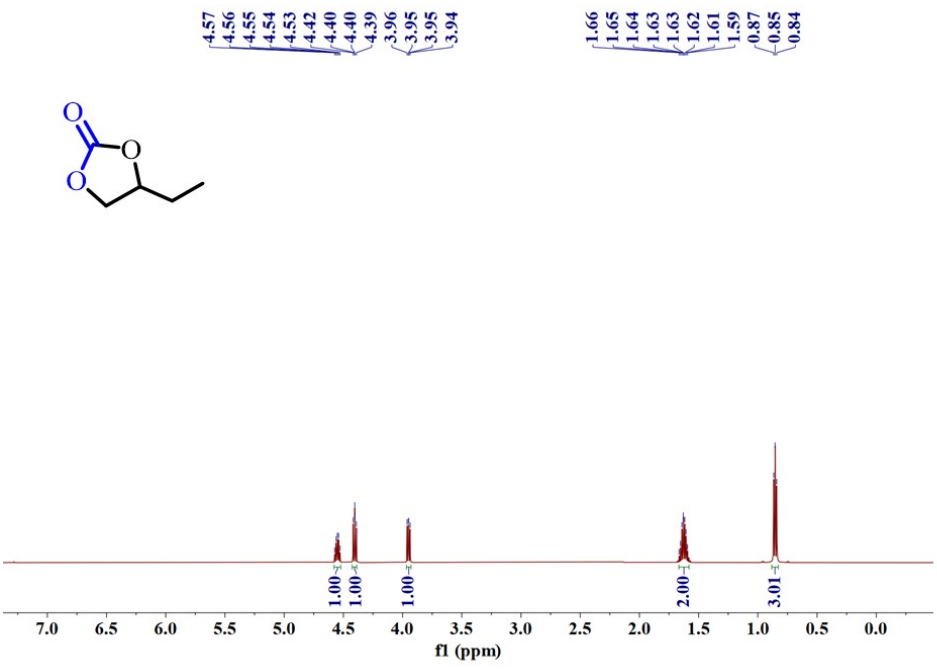

^{1}H NMR (600 MHz, $CDCl_3$) spectrum of 4b

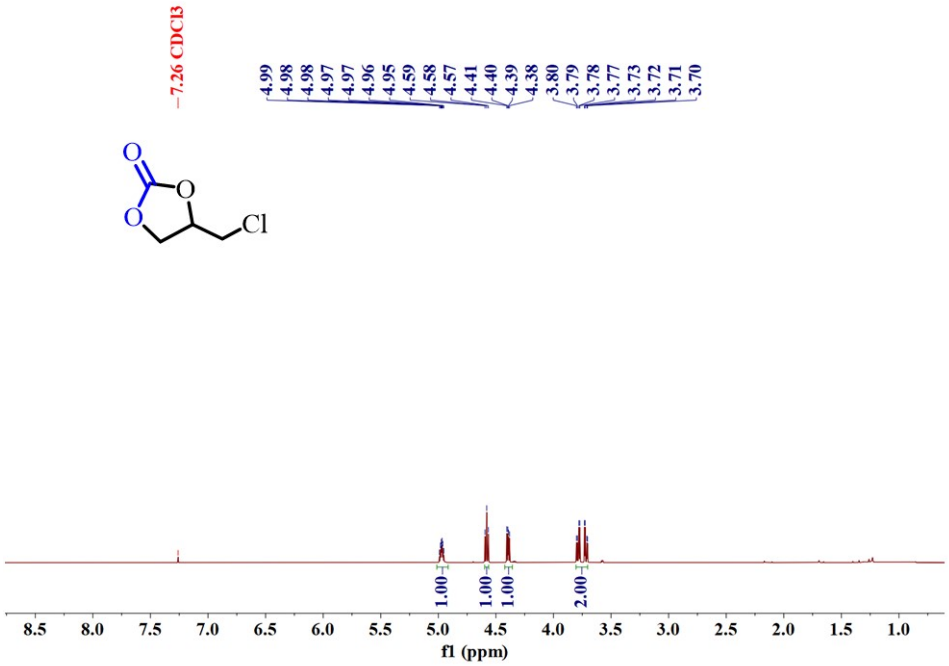

^{1}H NMR (600 MHz, $CDCl_3$) spectrum of 4c

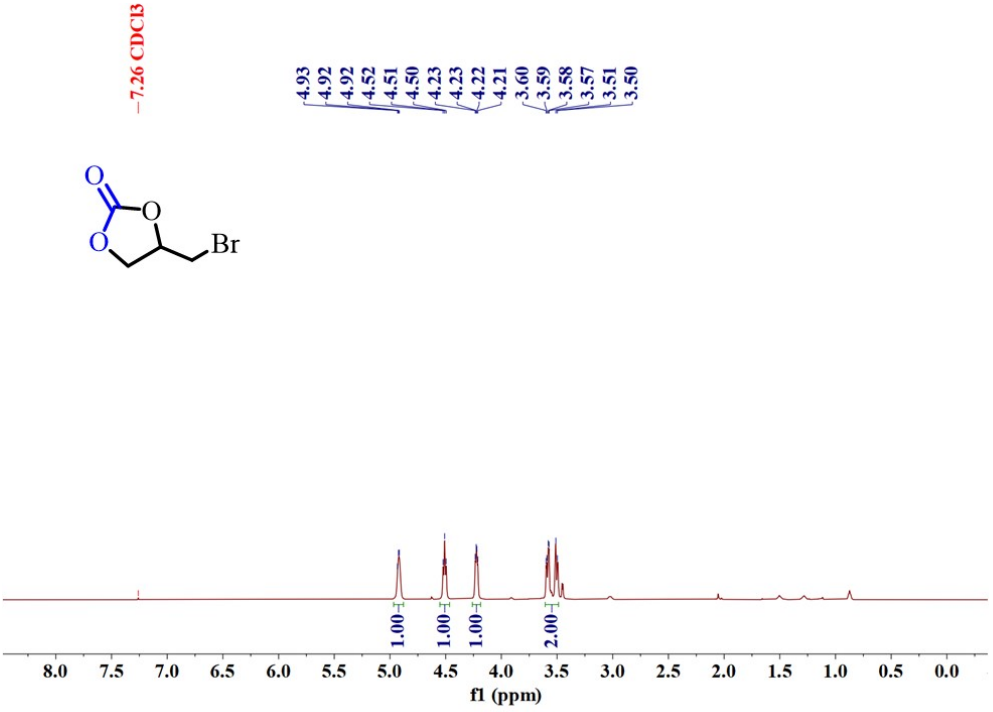

^{1}H NMR (600 MHz, $CDCl_3$) spectrum of 4d

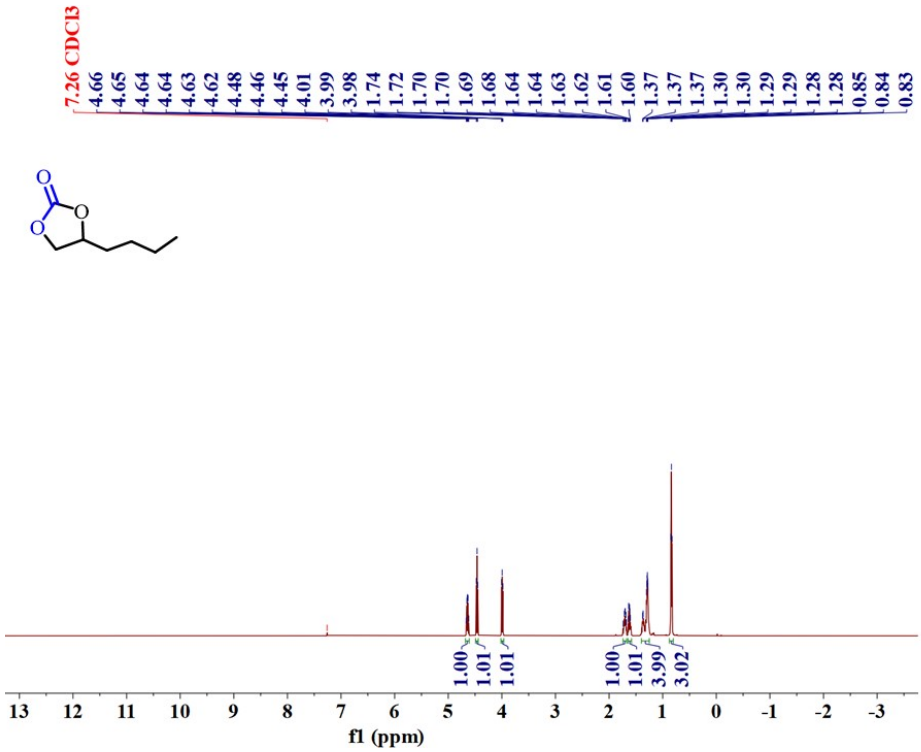

^{1}H NMR (600 MHz, $CDCl_3$) spectrum of 4e

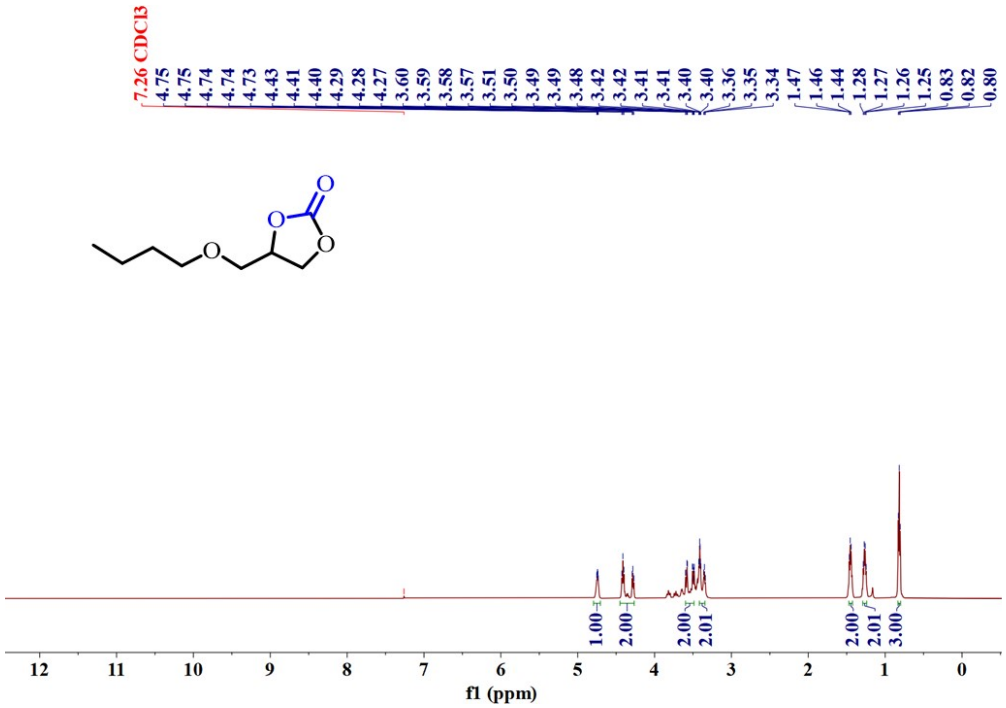

^{1}H NMR (600 MHz, $CDCl_3$) spectrum of 4f

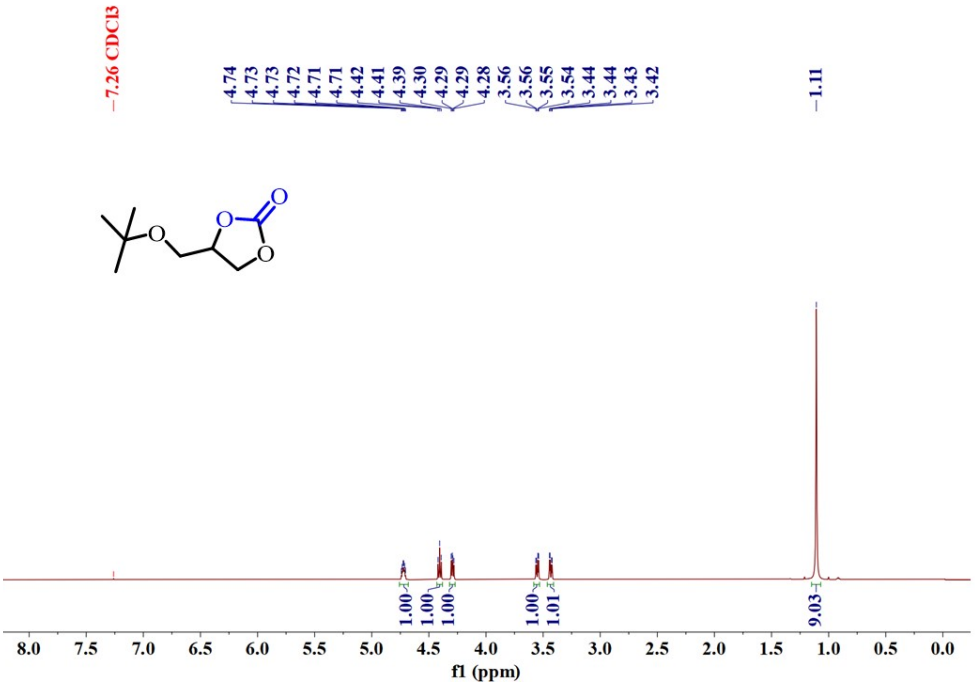

^{1}H NMR (600 MHz, $CDCl_3$) spectrum of 4g

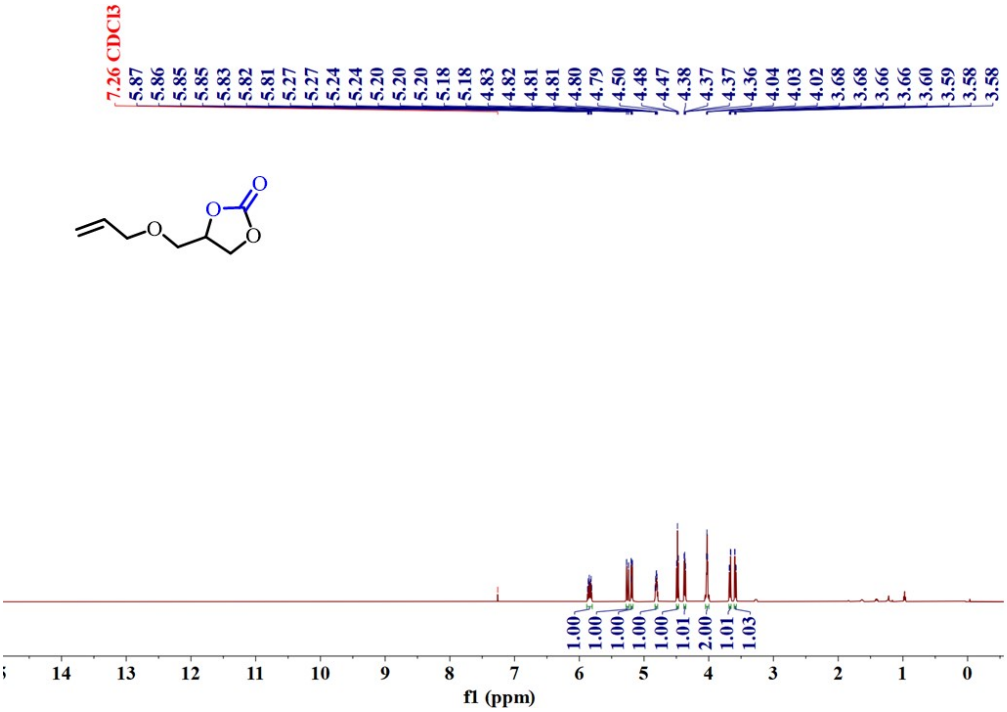

^{1}H NMR (600 MHz, $CDCl_3$) spectrum of 4h

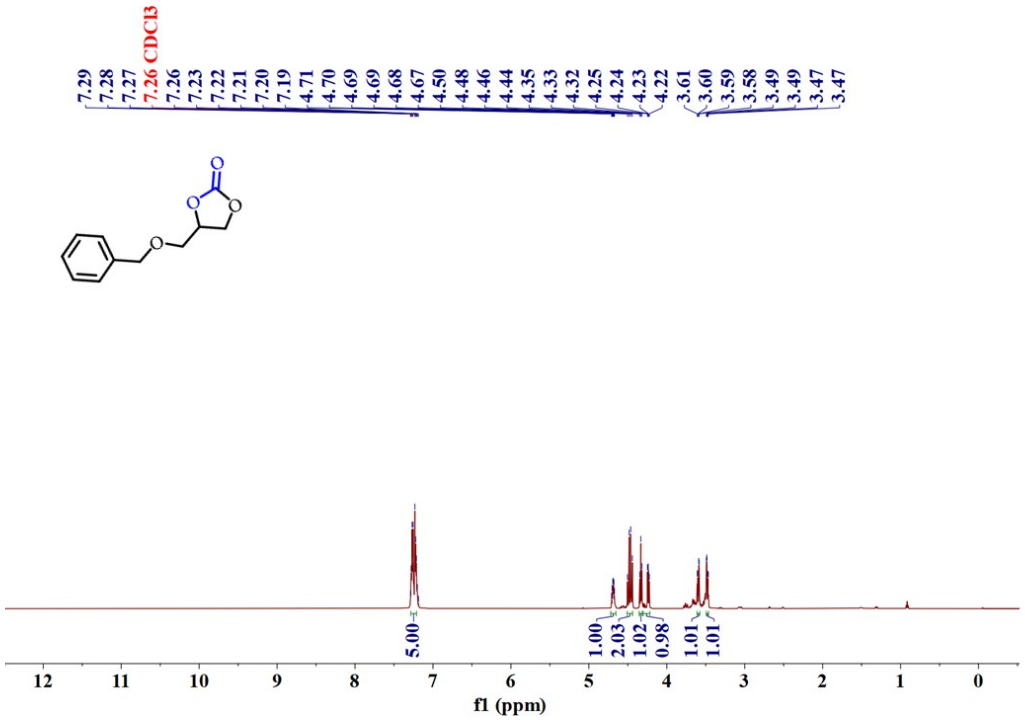

^{1}H NMR (600 MHz, $CDCl_3$) spectrum of 4i

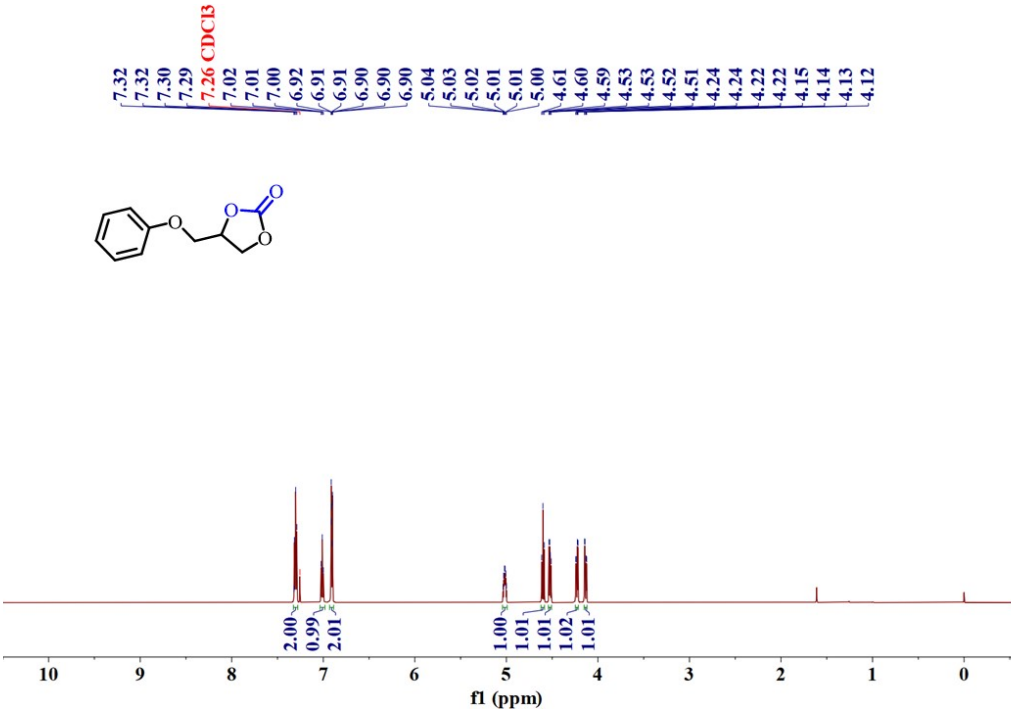

^{1}H NMR (600 MHz, $CDCl_3$) spectrum of 4j

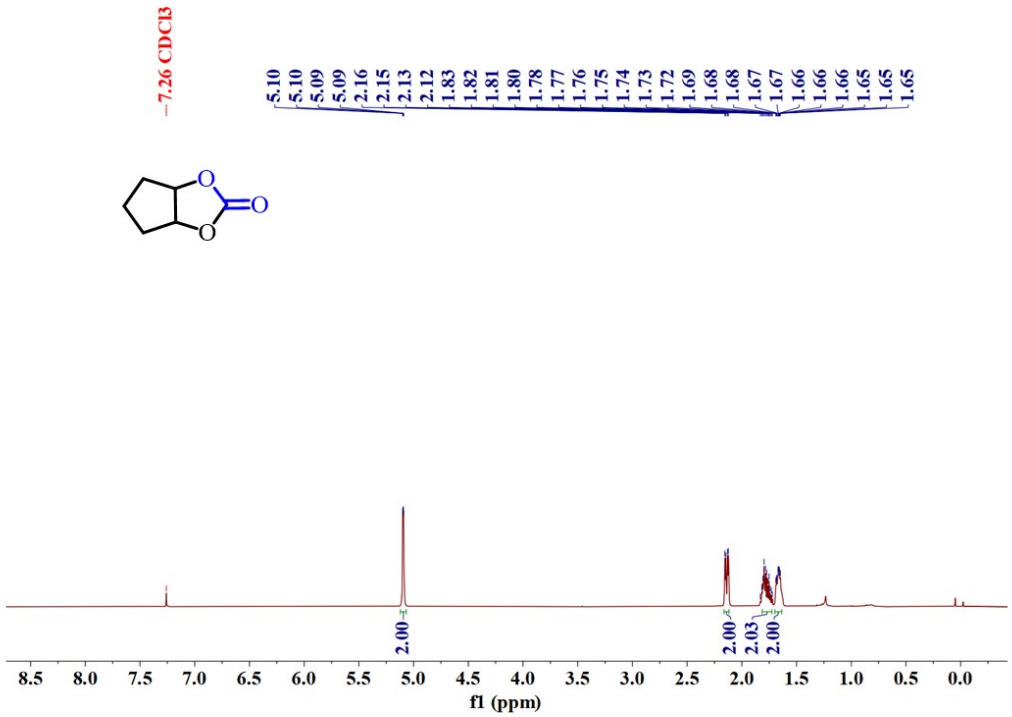

^{1}H NMR (600 MHz, $CDCl_3$) spectrum of 4k

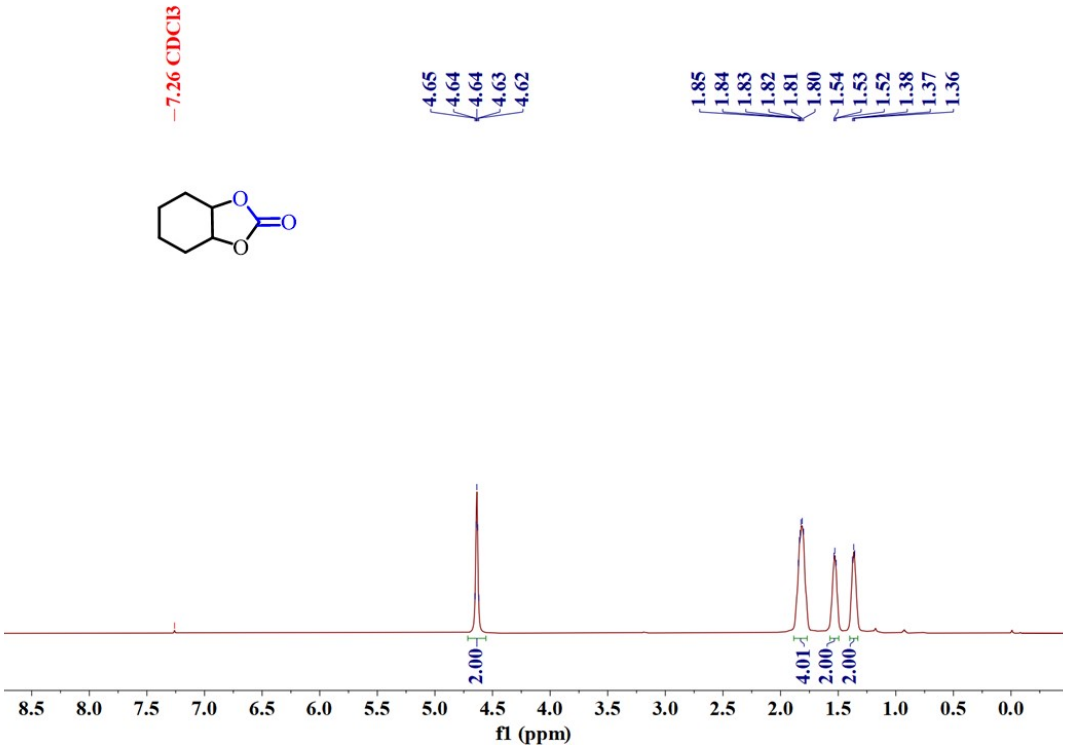

^{1}H NMR (600 MHz, $CDCl_3$) spectrum of 4l

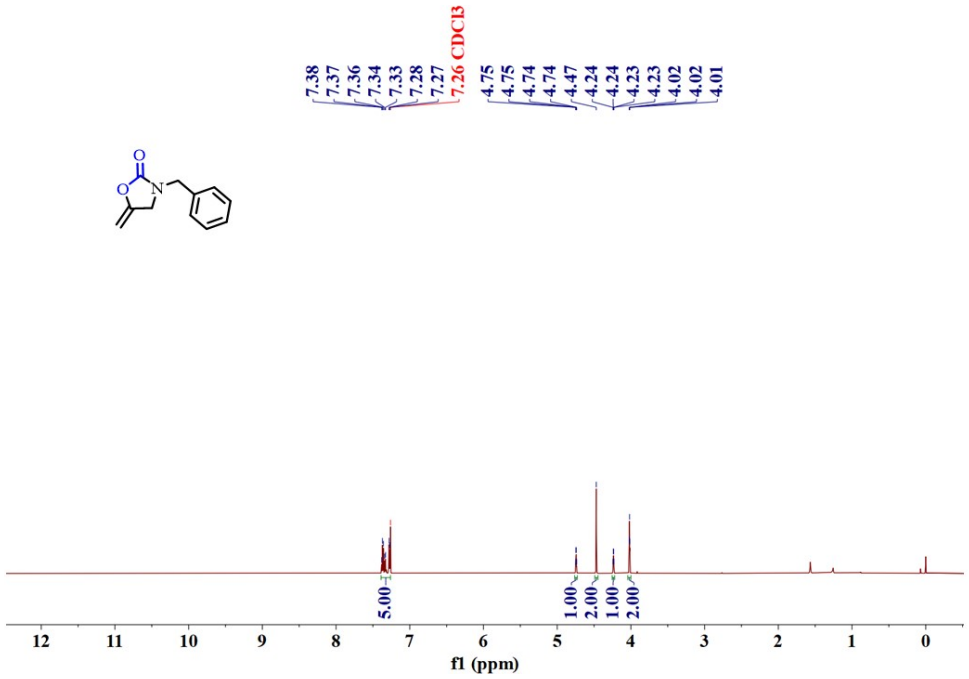

^{1}H NMR (600 MHz, $CDCl_3$) spectrum of 6a

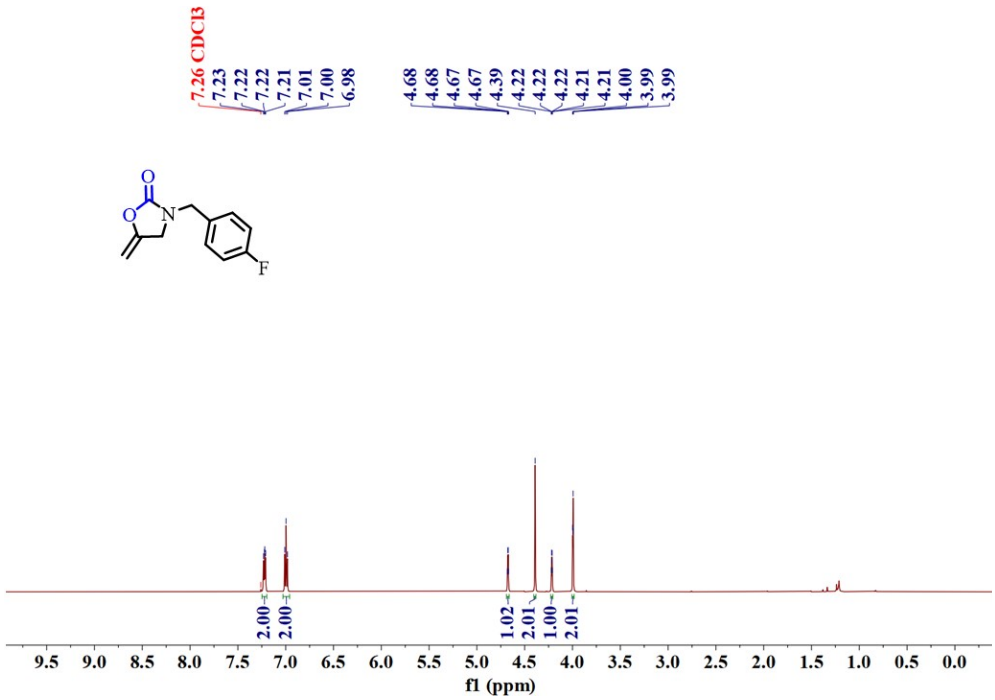

^{1}H NMR (600 MHz, $CDCl_3$) spectrum of 6b

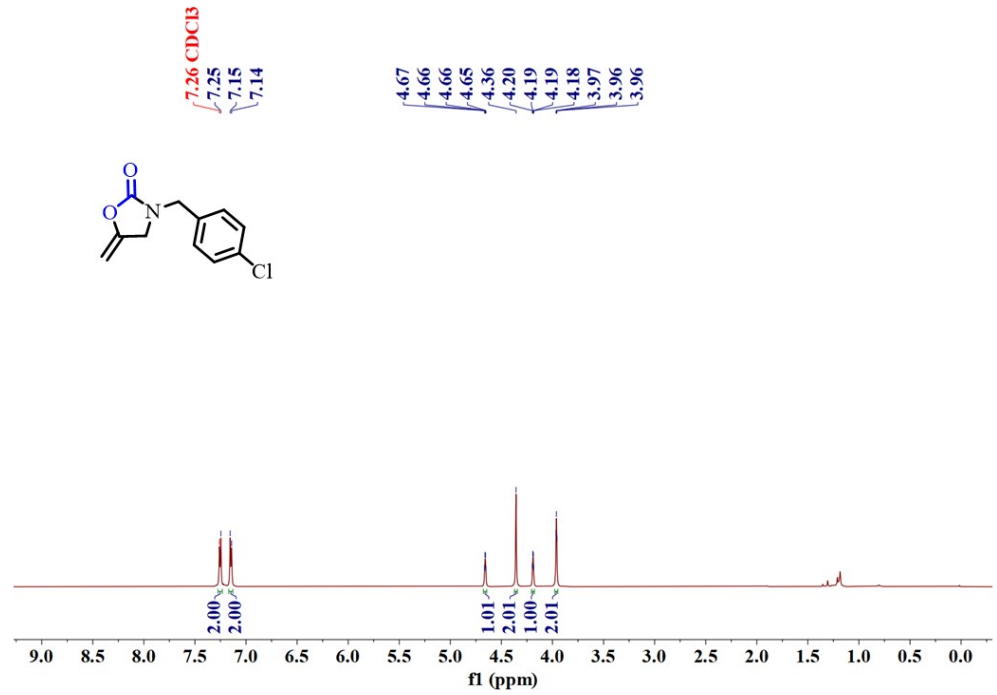

^{1}H NMR (600 MHz, $CDCl_3$) spectrum of 6c

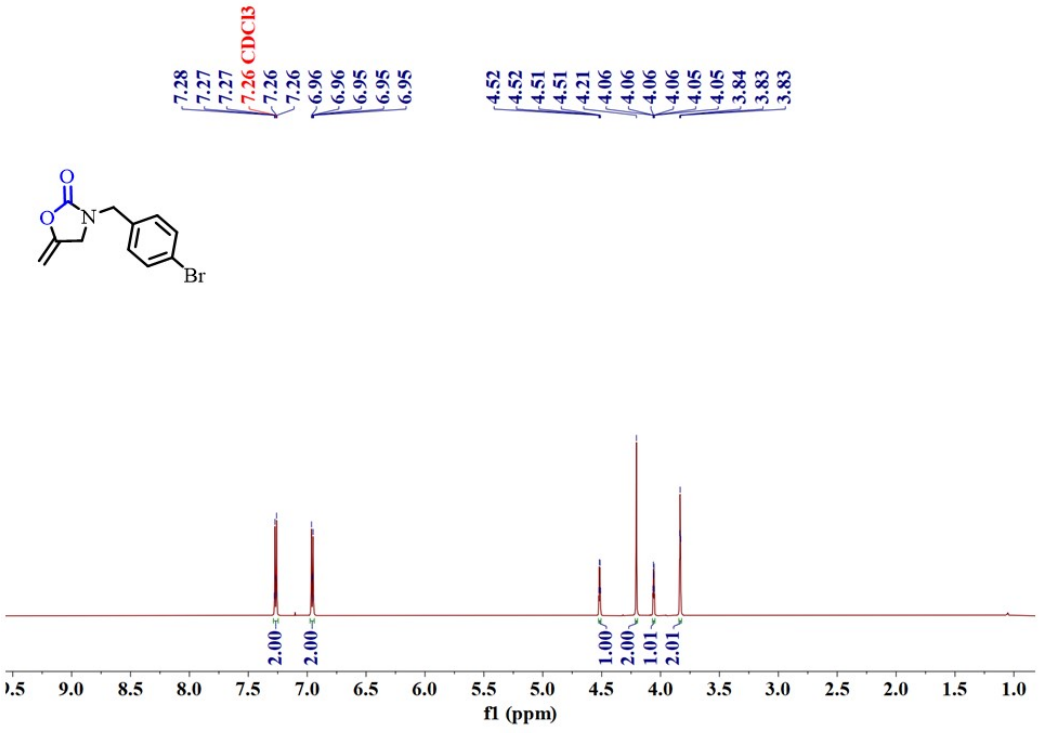

^{1}H NMR (600 MHz, $CDCl_3$) spectrum of 6d

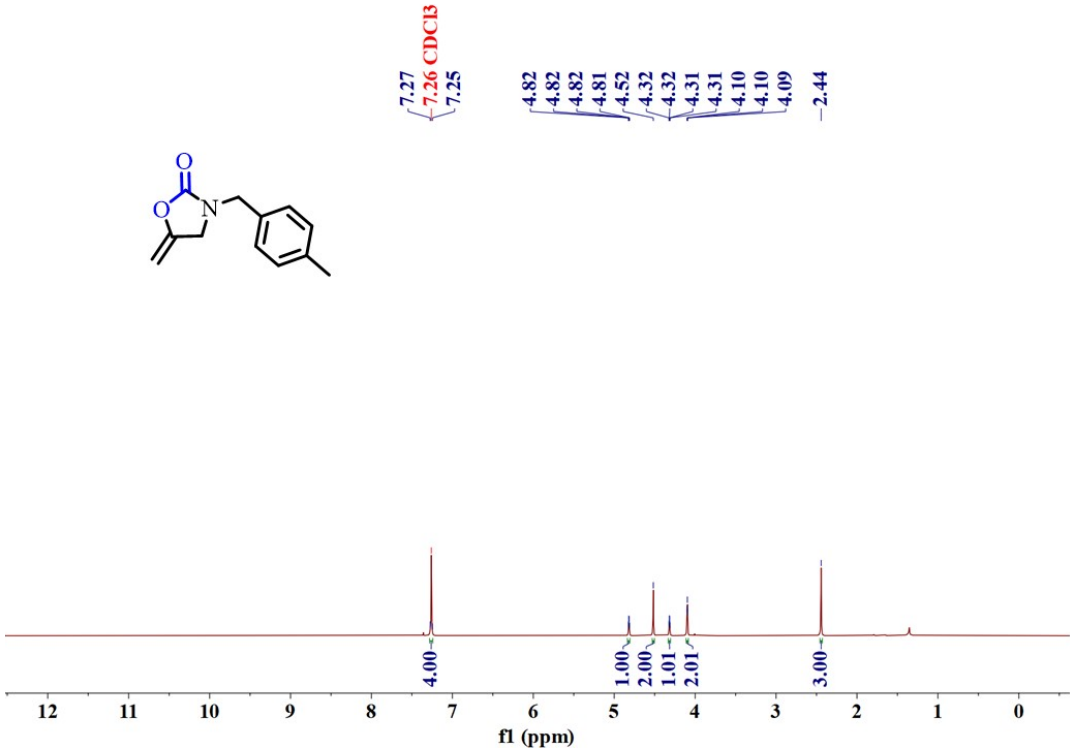

^{1}H NMR (600 MHz, $CDCl_3$) spectrum of 6e

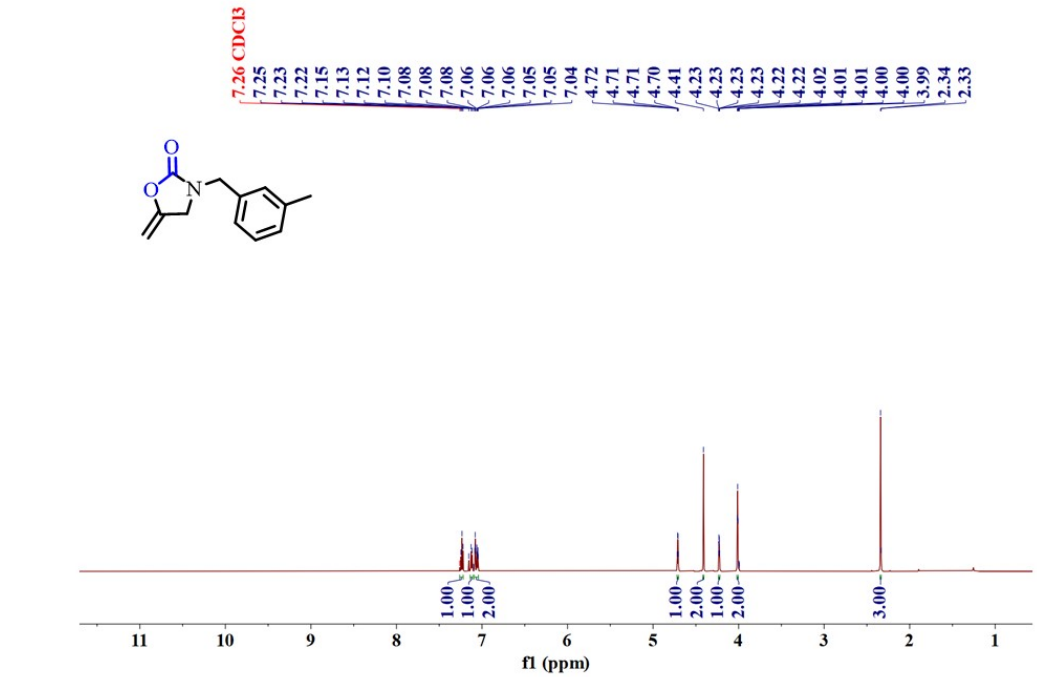

^{1}H NMR (600 MHz, $CDCl_3$) spectrum of 6f

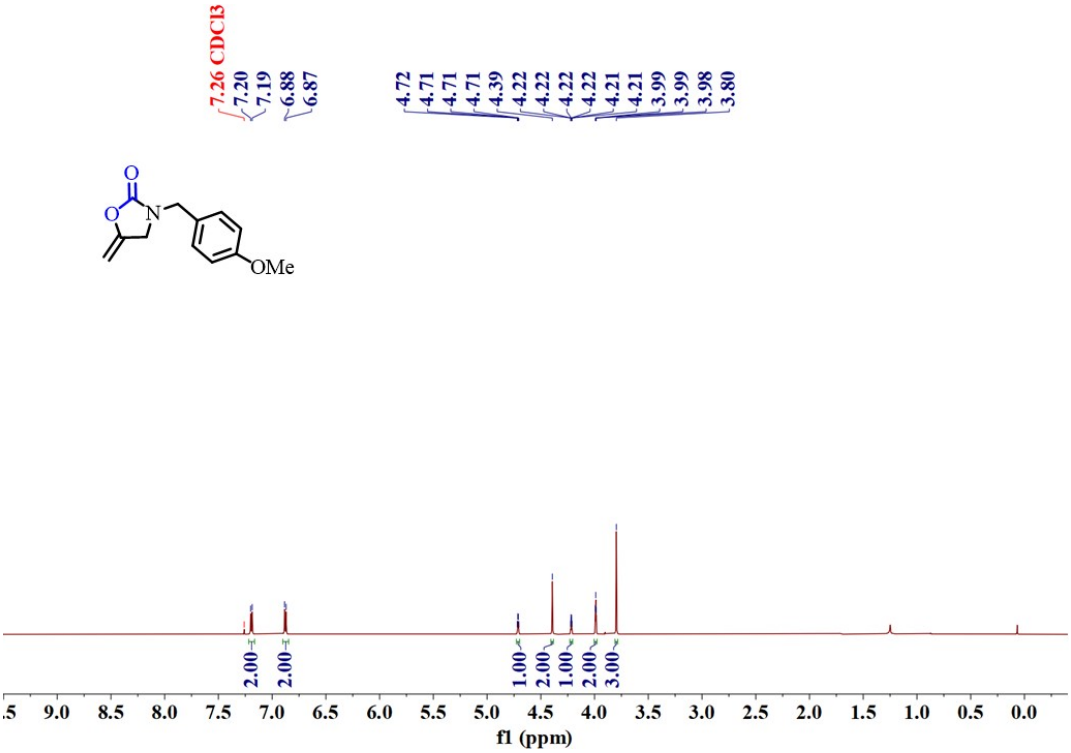

^{1}H NMR (600 MHz, $CDCl_3$) spectrum of 6g

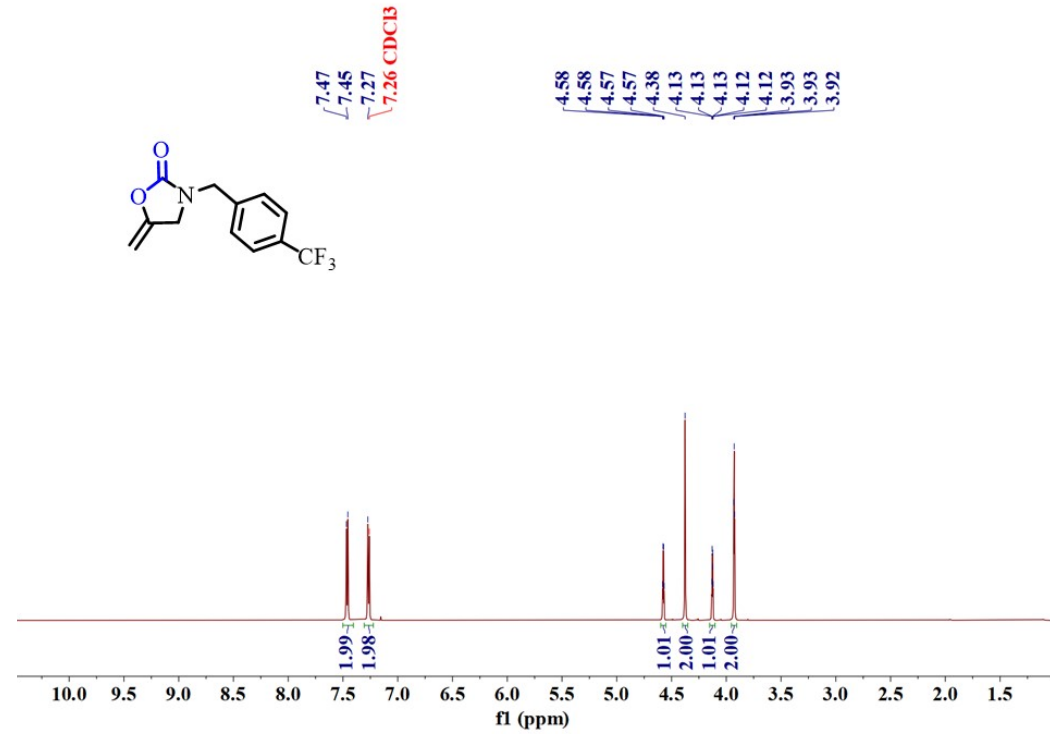

^{1}H NMR (600 MHz, $CDCl_3$) spectrum of 6h

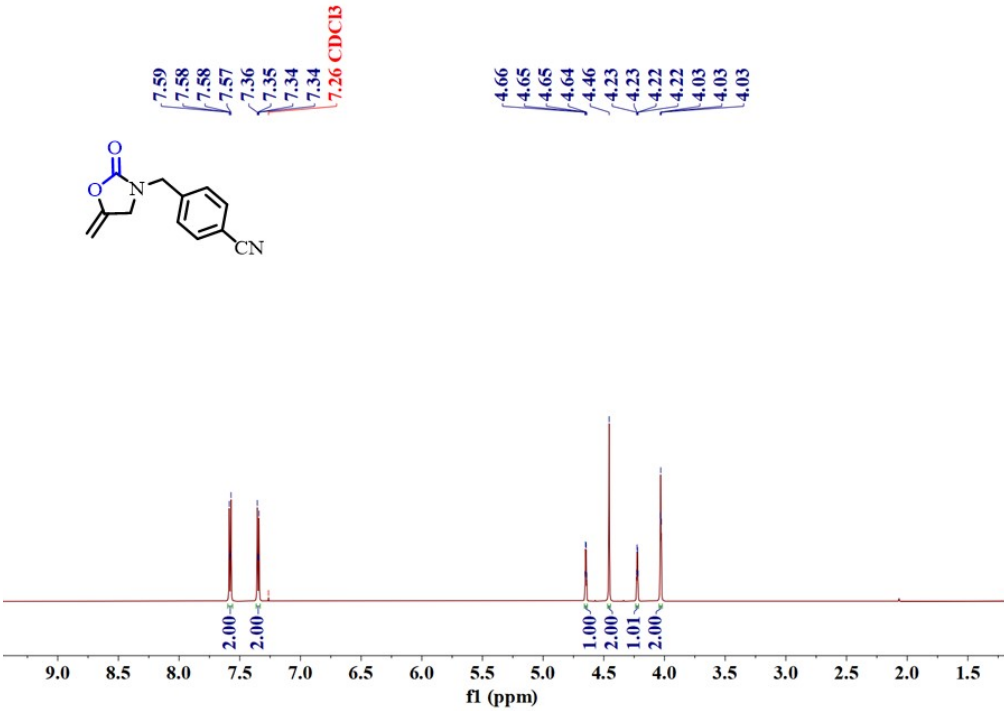

^{1}H NMR (600 MHz, $CDCl_3$) spectrum of 6i

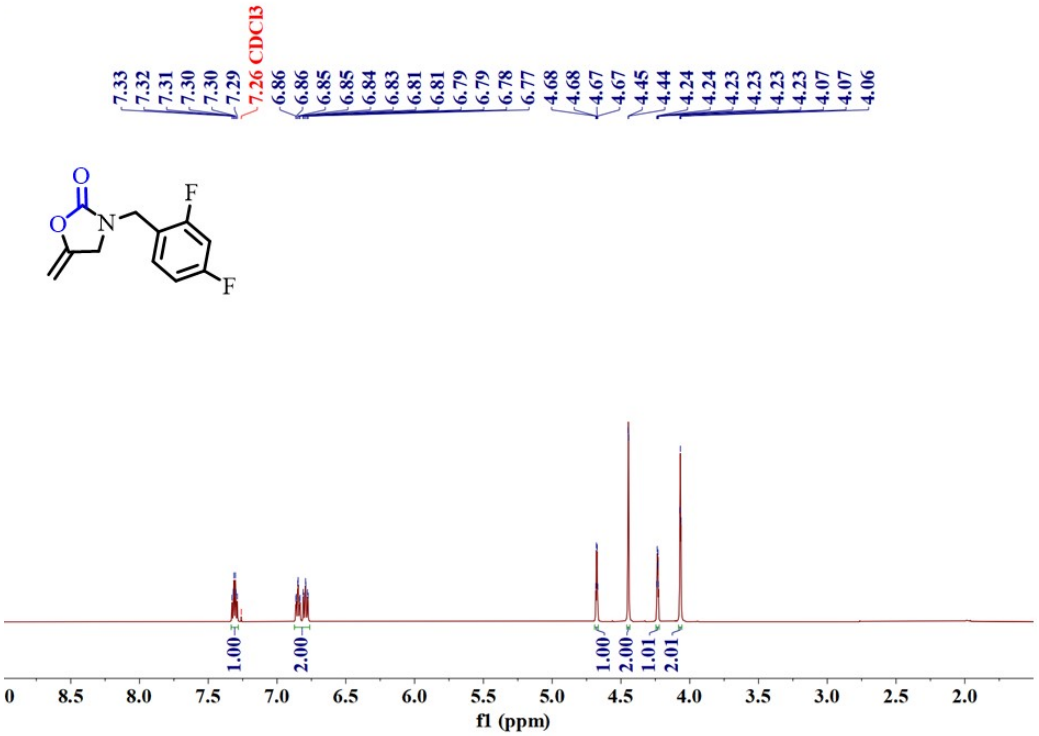

^{1}H NMR (600 MHz, $CDCl_3$) spectrum of 6j

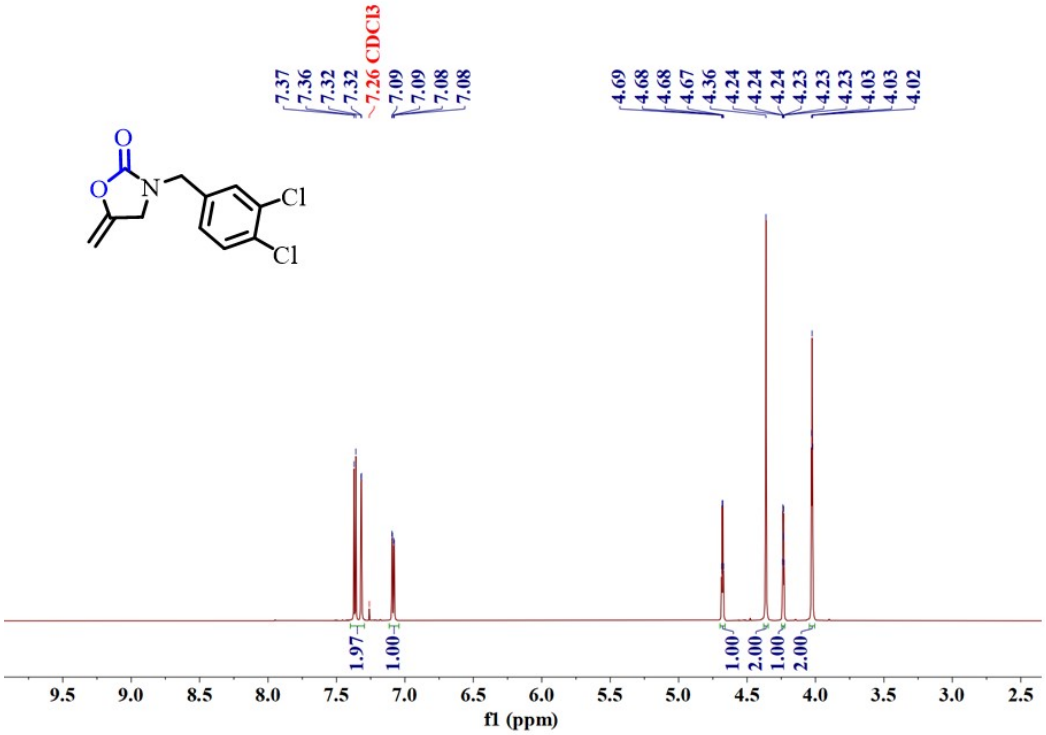

^{1}H NMR (600 MHz, $CDCl_3$) spectrum of 6k

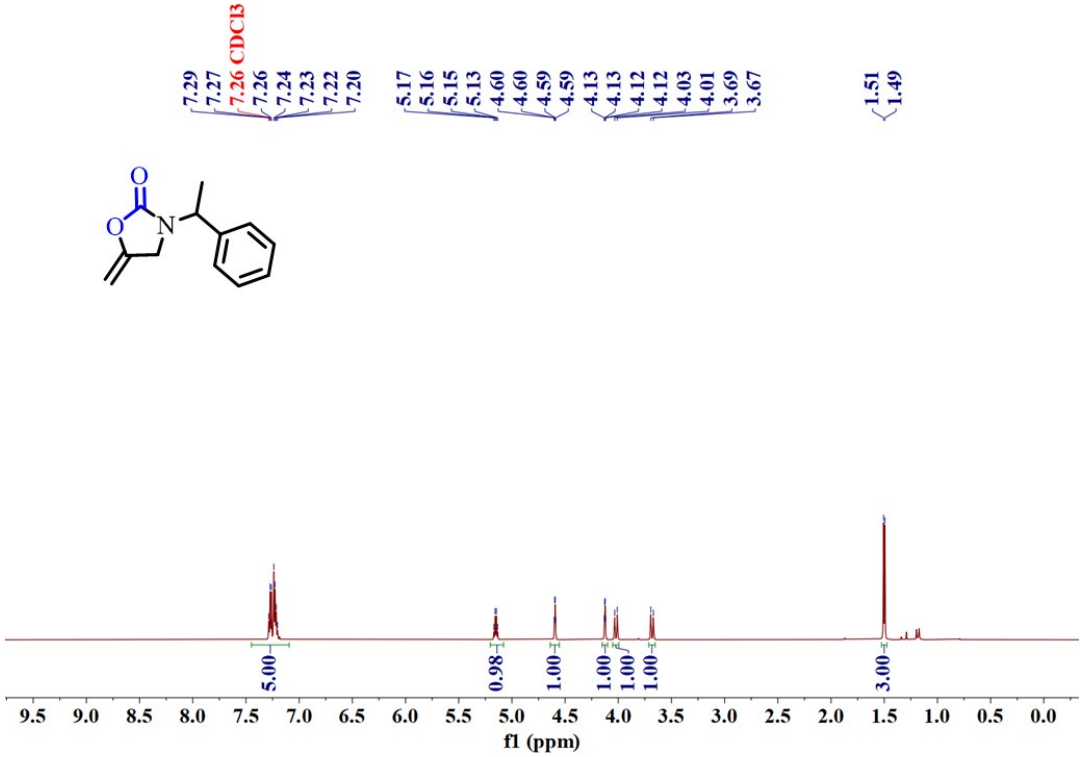

^{1}H NMR (600 MHz, $CDCl_3$) spectrum of 6l

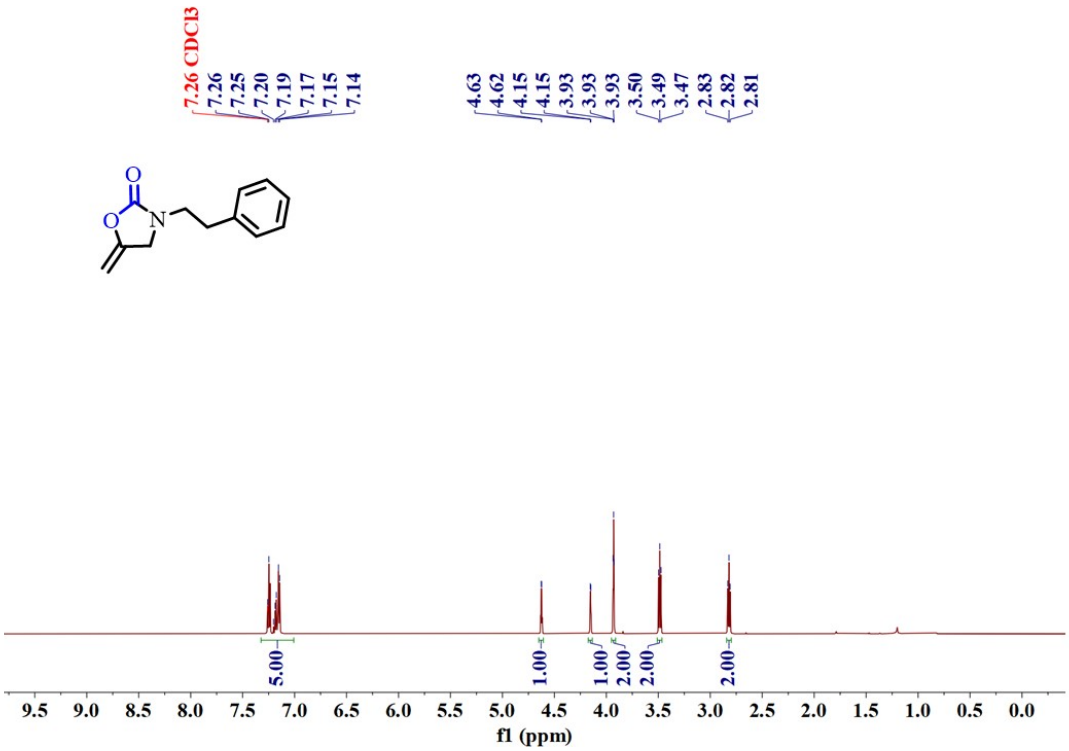

^{1}H NMR (600 MHz, $CDCl_3$) spectrum of 6m

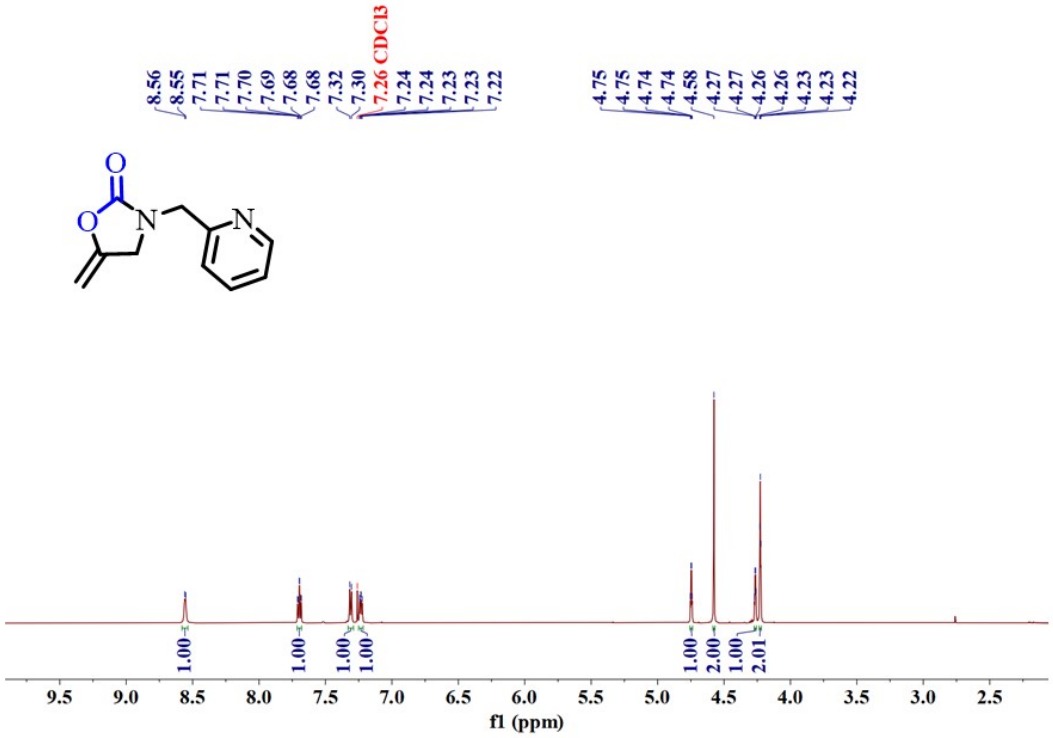

^{1}H NMR (600 MHz, $CDCl_3$) spectrum of 6n

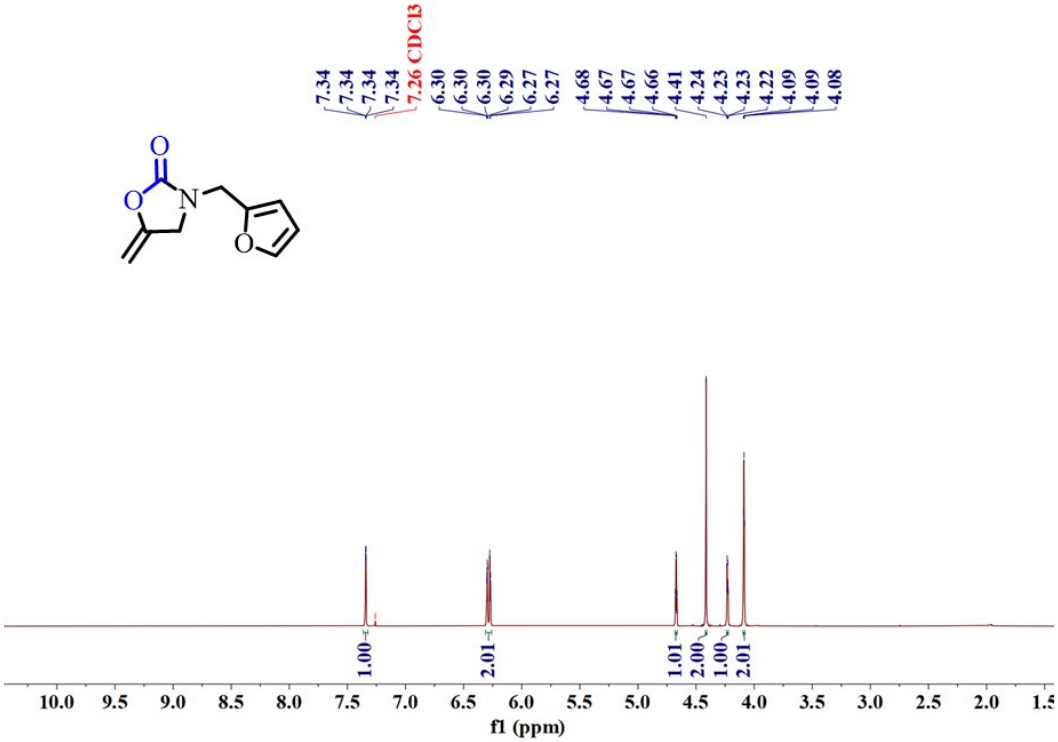

^{1}H NMR (600 MHz, $CDCl_3$) spectrum of 6o

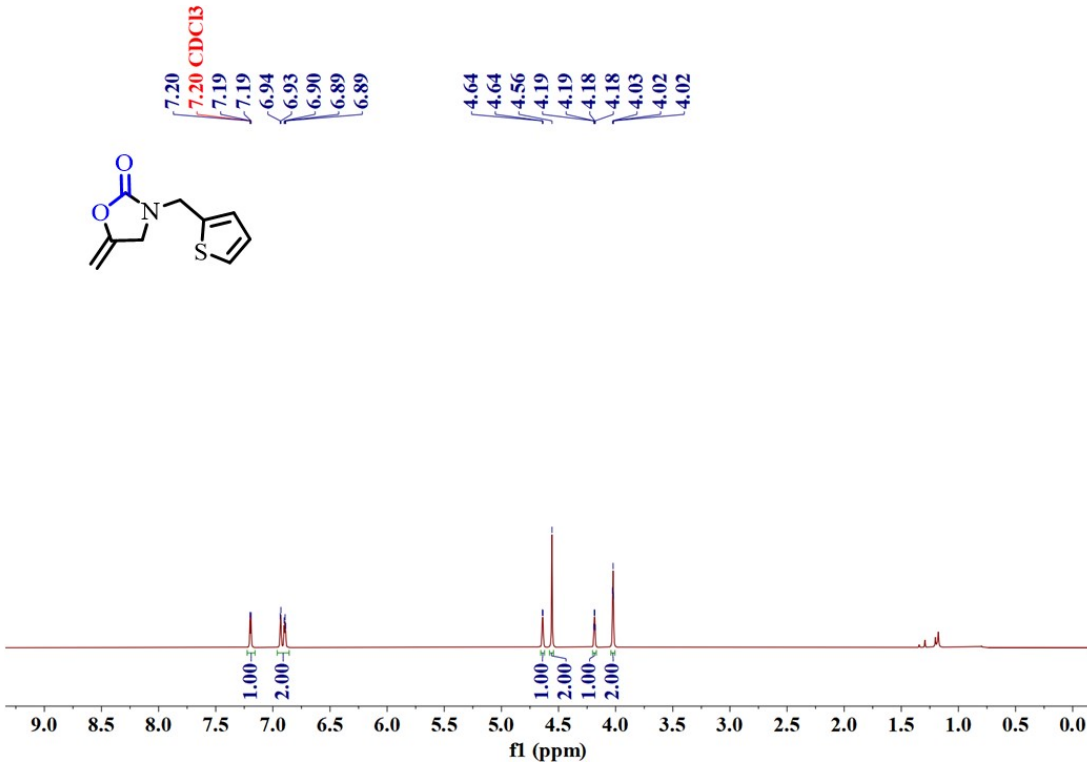

^{1}H NMR (600 MHz, $CDCl_3$) spectrum of 6p

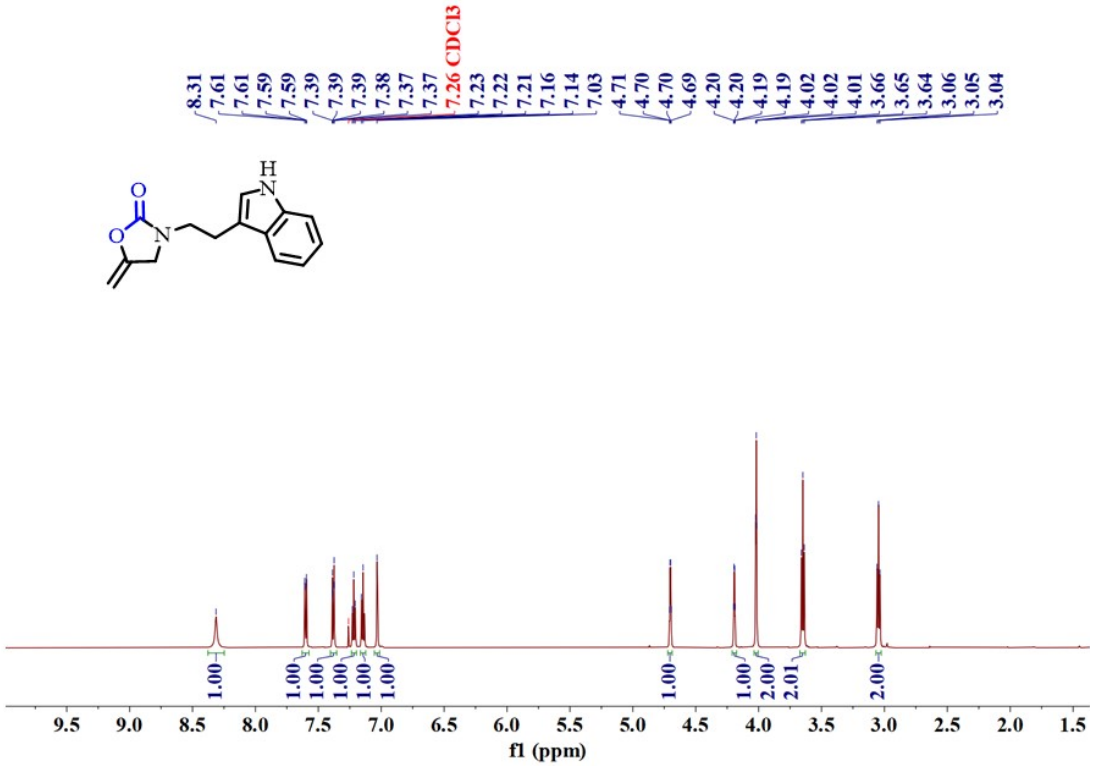

^{1}H NMR (600 MHz, $CDCl_3$) spectrum of 6q

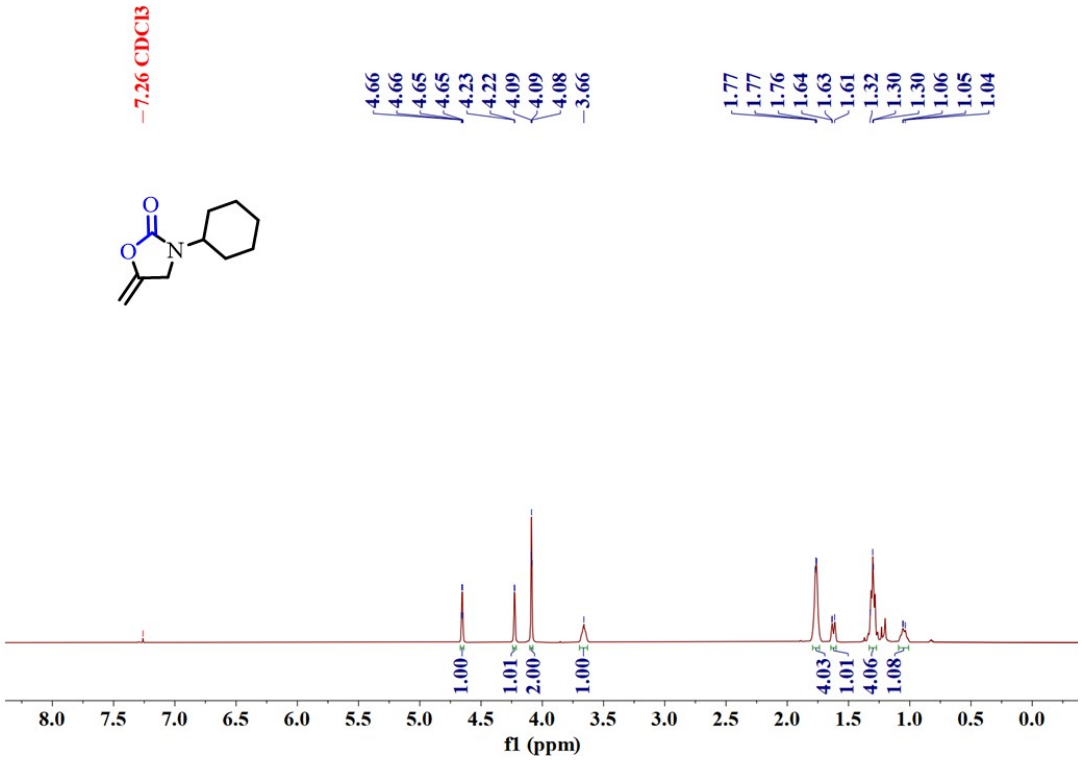

^{1}H NMR (600 MHz, $CDCl_3$) spectrum of 6r

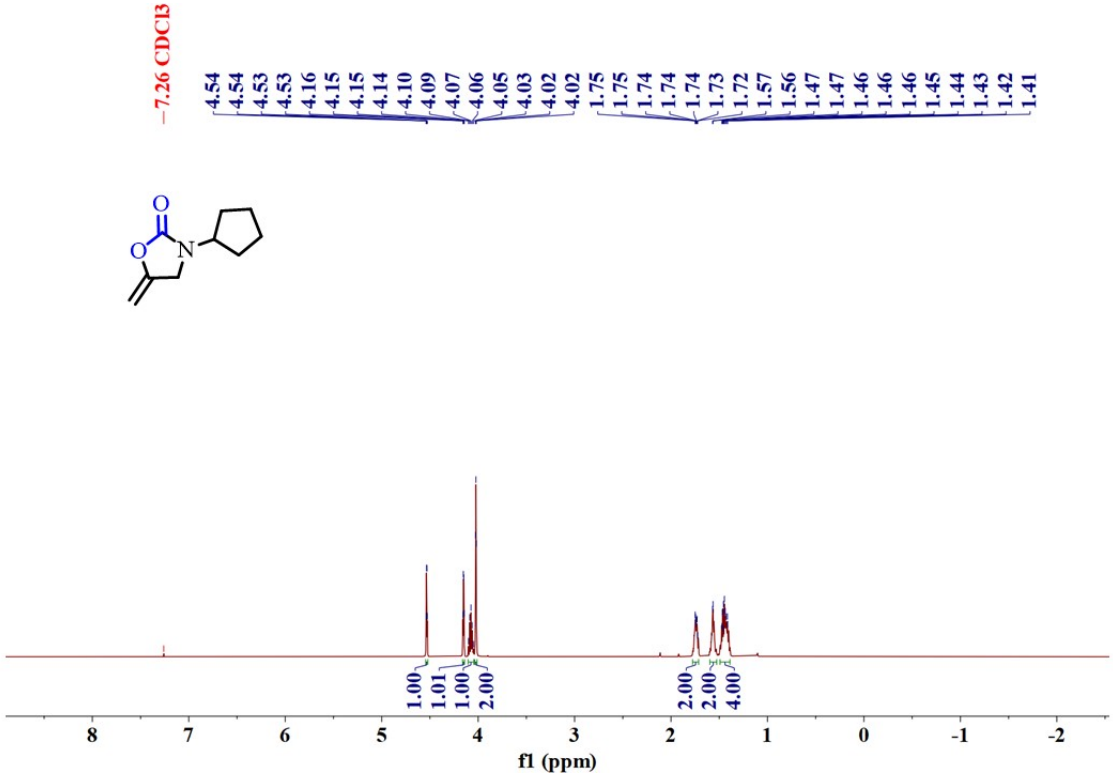

^{1}H NMR (600 MHz, $CDCl_3$) spectrum of 6s

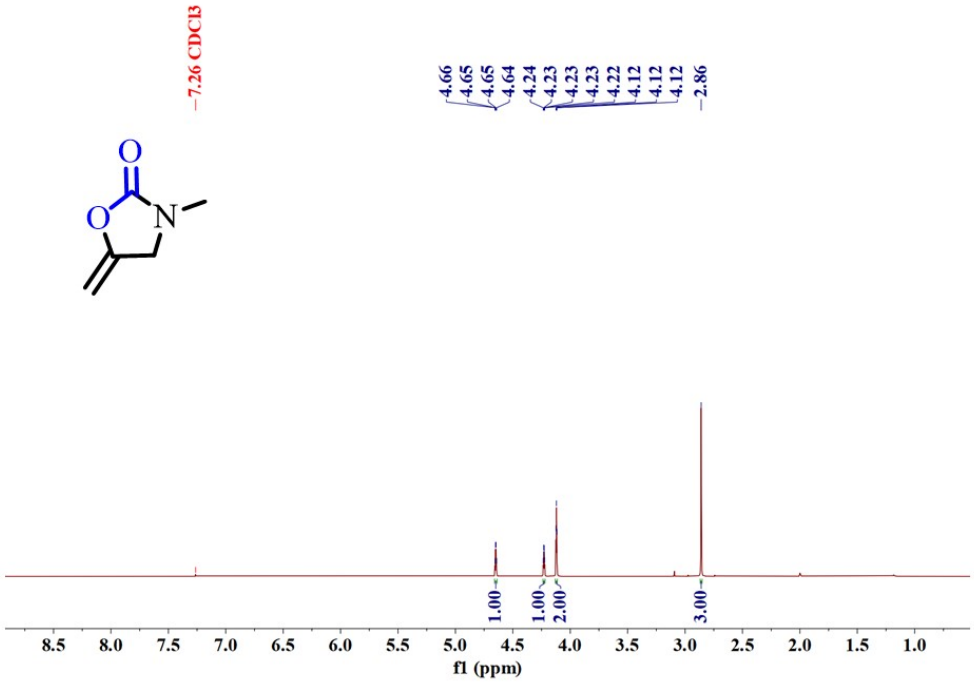

^{1}H NMR (600 MHz, $CDCl_3$) spectrum of 6t

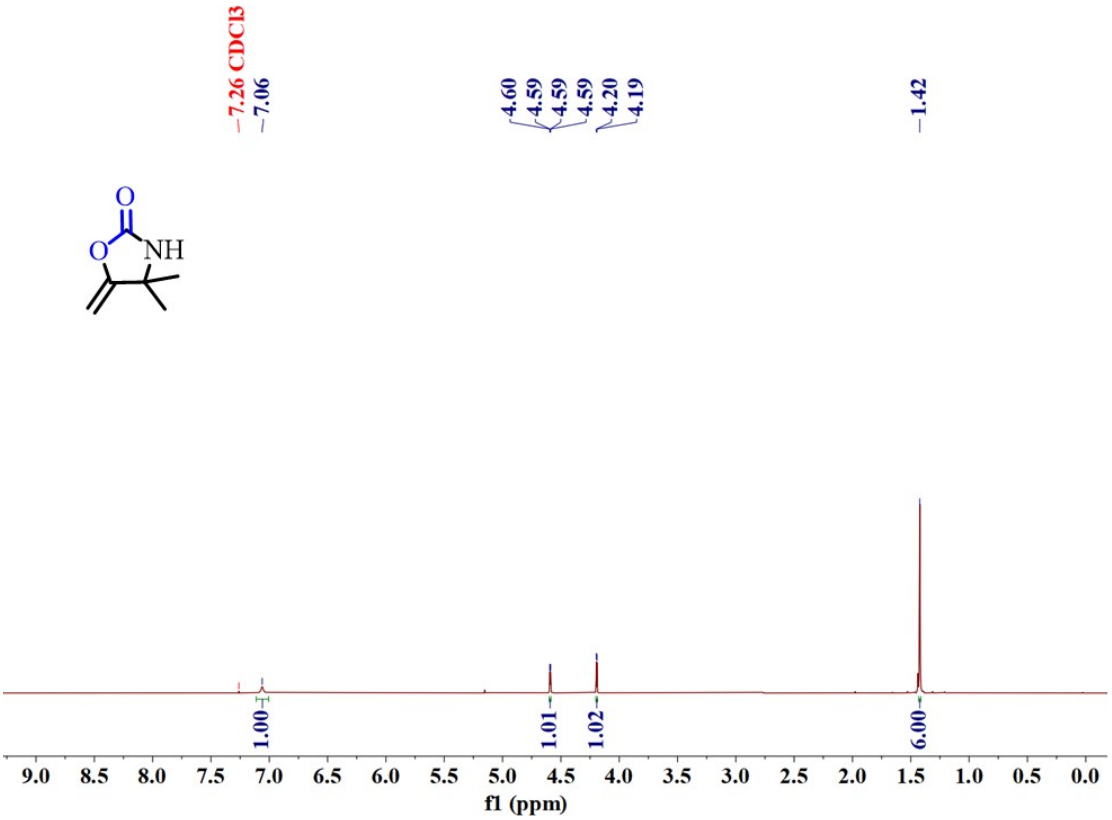

^{1}H NMR (600 MHz, $CDCl_3$) spectrum of 6u

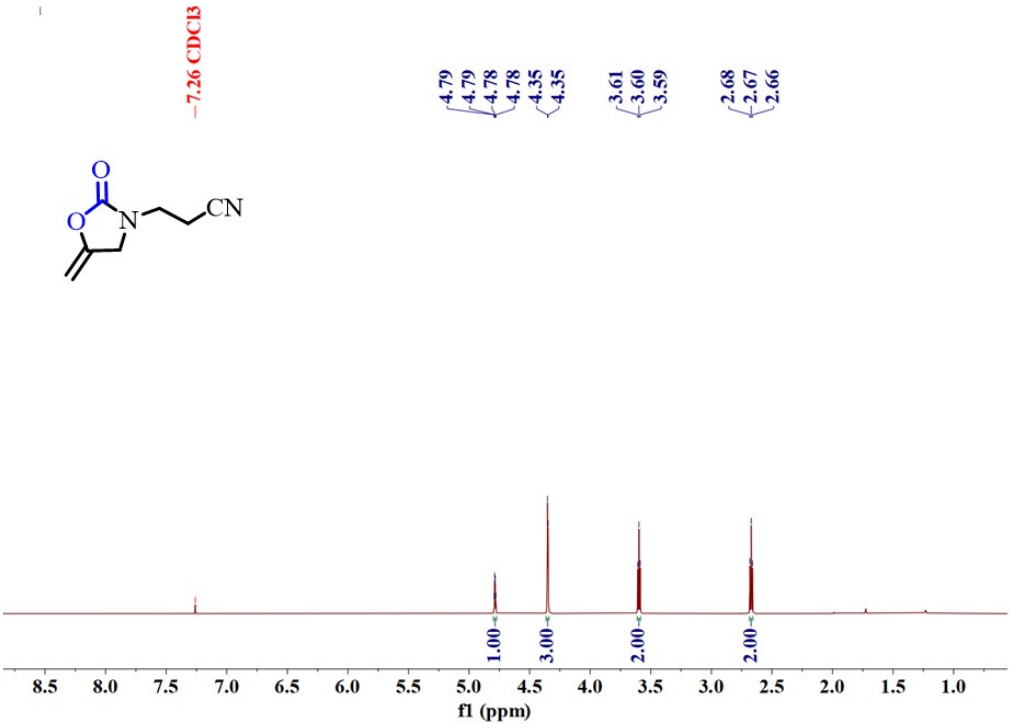

^{1}H NMR (600 MHz, $CDCl_3$) spectrum of 6v

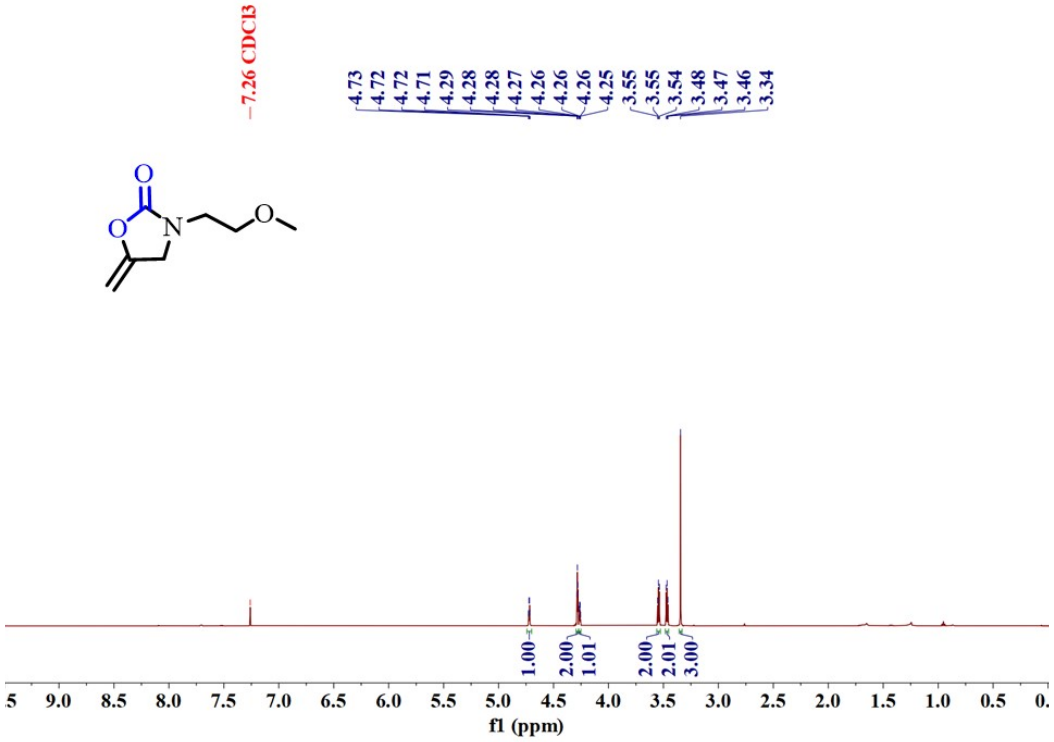

^{1}H NMR (600 MHz, $CDCl_3$) spectrum of 6w

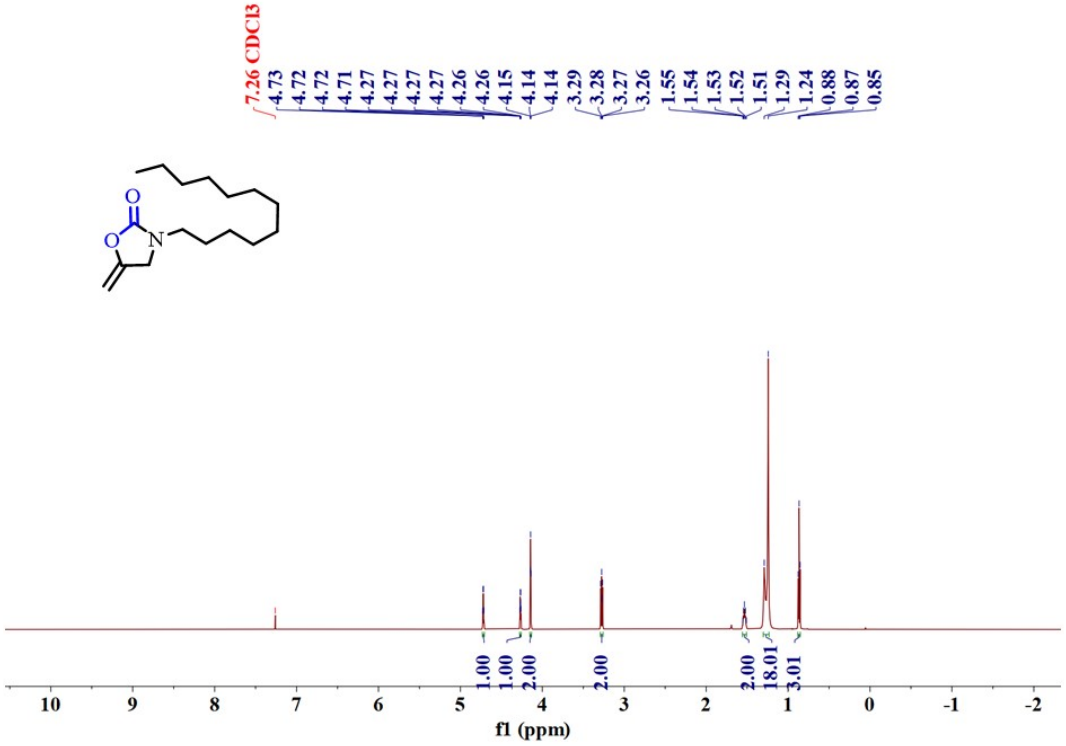

^{1}H NMR (600 MHz, $CDCl_3$) spectrum of 6x

References

1. O. V. Dolomanov, L. J. Bourhis, R. J. Gildea, J. A. K. Howard and H. Puschmann, *J. Appl.*

Cryst., 2009, **42**, 339-341.
2. G. M. Sheldrick, *Acta Cryst.*, 2015, **71**, 3-8.
3. G. M. Sheldrick, *Acta Cryst.*, 2015, **71**, 3-8.
4. Z. L. Ma, P. X. Liu, Z. Y. Liu, J. J. Wang, L. B. Li and L. Tian, *Inorg.Chem.*, 2021, **60**, 6550-6558.
5. R. A. Molla, K. Ghosh, B. Banerjee, M. A. Iqubal, S. K. Kundu, S. M. Islam and A. Bhaumik, *J. Colloid Interface Sci.*, 2016, **477**, 220-229.
6. G. Singh, N. Duhan, T. J. Dhilip Kumar and C. M. Nagaraja, *ACS Appl. Mater. Interfaces*, 2024, **16**, 5857-5868.
7. G. Shi, W. Xu, J. Wang, Y. Yuan, S. Chaemchuen and F. Verpoort, *J. CO_2 Util.*, 2020, **39**.
8. R.-J. Wei, M. Xie, R.-Q. Xia, J. Chen, H.-J. Hu, G.-H. Ning and D. Li, *J. Am. Chem. Soc.*, 2023, **145**, 22720-22727.
9. Y. Wang, J. Zhang, S. Wang, Z. Tan, Y. Yang, Y. Zhao, B. Han, Q. Li and J. Xiang, *ACS Cata.*, 2024, **14**, 18397-18405.
10. P. Jing, B. Wu, Z. Han, W. Shi and P. Cheng, *Chin. Chem. Lett.*, 2021, **32**, 3505-3508.
11. N.-N. Zhu, X.-H. Liu, T. Li, J.-G. Ma, P. Cheng and G.-M. Yang, *Inorg. Chem.*, 2017, **56**, 3414-3420.
12. P. Liu, T. Zhao, F. Zhao, Z. Xu, Y. Huang and X. Hu, *Adv. Funct. Mater.*, 2025, 2508657.
13. L. Kan, L. Zhang, L. Z. Dong, X. H. Wang, R. H. Li, C. Guo, X. Li, Y. Yan, S. L. Li and Y. Q. Lan, *Adv. Mater*, 2024, **36**, 2310061.
14. C.-Y. Tsai, Y.-H. Chen, S. Lee, C.-H. Lin, C.-H. Chang, W.-T. Dai and W.-L. Liu, *Inorg. Chem.*, 2022, **61**, 2724-2732.
15. X. Qin, X. Yu, J. Si, S. Xie, Z. Shi, X. Liu, C. Li, G. Li and Y. Liu, *Chem. Eng. J*, 2025, **516**, 163674.
16. F. Li, J. Wang, X.-K. Zhang, B.-J. Yao and Y.-B. Dong, *Chem. Commun.*, 2025, **61**, 16806-16809.
17. X. Si, Q. Yao, X. Pan, X. Zhang, C. Zhang, Z. Li, W. Duan, J. Hou and X. Huang, *Inorg. Chem.*, 2023, **62**, 15006-15014.
18. X. Wang, J. Li, M. Kou, W. Dou, D. Bai, X. Tang, Y. Tang and W. Liu, *Inorg. Chem.*, 2023, **62**, 19015-19024.
19. H.-Q. Yin, M.-Y. Cui, H. Wang, Y.-Z. Peng, J. Chen, T.-B. Lu and Z.-M. Zhang, *Inorg. Chem.*, 2023, **62**, 13722-13730.
20. J. Ye, T. Chen, N. Chai, Q. Jiang, Q. Guo, F.-Y. Yi and X. Ma, *Cryst. Growth Des.,* 2025, **25**, 2903-2912.
21. P. Jiang, L. Ma, K. Wang, K. Lan, Z. Zhan, A. Iqbal, F. Niu and R. Li, *New J. Chem.,* 2019, **43**, 17211-17219.
22. Y.-M. Wang, K.-M. Mo, D. Luo, M.-X. Tao, X. Chen, G.-H. Ning and D. Li, *Inorg. Chem. Front.*, 2024, **11**, 6072-6078.
23. M.-H. Tang, Y.-C. Wang, Z. Fang, L.-H. Duan, J.-Z. Han, S.-H. Jing, M. Zhou, F.-Y. Ren, J. Zhao, H. Xu and B. Zhao, *Inorg. Chem.*, 2025, **64**, 2537-2544.
24. C. S. Cao, S. M. Xia, Z. J. Song, H. Xu, Y. Shi, L. N. He, P. Cheng and B. Zhao, *Angew. Chem. Int. Ed.*, 2020, **59**, 8586-8593.
25. X. Chen, J.-Y. Song, J. Zheng, Y.-M. Wang, J. Luo, P. Weng, B.-C. Cai, X.-C. Lin, G.-H. Ning and D. Li, *J. Am. Chem. Soc.*, 2024, **146**, 19271-19278.

26. Z.-W. Zheng, J.-J. Zhou, H. Liu, X.-Y. Zhang, J. Zhao, D.-S. Zheng, K. Huang and D.-B. Qin, *Inorg. Chem.*, 2024, **63**, 16878-16887.
27. S. Ghosh, P. Laha, N. U. D. Mir, P. Das, P.-R. Cha and S. Biswas, *Inorg. Chem.,* 2024, **63**, 21450-21461.
28. A. L. Gu, Y. X. Zhang, Z. L. Wu, H. Y. Cui, T. D. Hu and B. Zhao, *Angew. Chem. Int. Ed.*, 2022, **61**, e202114817.
29. M. Zhao, S. Huang, Q. Fu, W. Li, R. Guo, Q. Yao, F. Wang, P. Cui, C. H. Tung and D. Sun, *Angew. Chem. Int. Ed.*, 2020, **59**, 20031-20036.
30. N. N. Liu, Y. F. Li, J. Zheng, B. j. Liu, G.-N. Liu, Y. Wang, and S. Wang, *Inorg. Chem.,* 2025, 64, 4534–4543.